Fish and Shellfish Immunology 146 (2024) 109357

Contents lists available at ScienceDirect

Fish and Shellfish Immunology

journal homepage: www.elsevier.com/locate/fsi

Full length article

Mapping the cellular landscape of Atlantic salmon head kidney by single cell and single nucleus transcriptomics

Adriana M.S. Andresen [a,1], Richard S. Taylor [b,1], Unni Grimholt [a], Rose Ruiz Daniels [b], Jianxuan Sun [b], Ross Dobie [c], Neil C. Henderson [c,d], Samuel A.M. Martin [e], Daniel J. Macqueen [b,1,*], Johanna H. Fosse [a,1,**]

[a] Norwegian Veterinary Institute, Ås, Norway
[b] The Roslin Institute and Royal (Dick) School of Veterinary Studies, University of Edinburgh, Edinburgh, United Kingdom
[c] Centre for Inflammation Research, The Queen's Medical Research Institute, Edinburgh BioQuarter, University of Edinburgh, Edinburgh, United Kingdom
[d] MRC Human Genetics Unit, Institute of Genetics and Cancer, University of Edinburgh, Edinburgh, United Kingdom
[e] Scottish Fish Immunology Research Centre, School of Biological Sciences, University of Aberdeen, Aberdeen, United Kingdom

ARTICLE INFO

Keywords:
Atlantic salmon
Single cell RNA sequencing
Single nucleus RNA sequencing
Cellular heterogeneity
Head kidney
Marker genes

ABSTRACT

Single-cell transcriptomics is the current gold standard for global gene expression profiling, not only in mammals and model species, but also in non-model fish species. This is a rapidly expanding field, creating a deeper understanding of tissue heterogeneity and the distinct functions of individual cells, making it possible to explore the complexities of immunology and gene expression on a highly resolved level. In this study, we compared two single cell transcriptomic approaches to investigate cellular heterogeneity within the head kidney of healthy farmed Atlantic salmon (*Salmo salar*). We compared 14,149 cell transcriptomes assayed by single cell RNA-seq (scRNA-seq) with 18,067 nuclei transcriptomes captured by single nucleus RNA-Seq (snRNA-seq). Both approaches detected eight major cell populations in common: granulocytes, heamatopoietic stem cells, erythrocytes, mononuclear phagocytes, thrombocytes, B cells, NK-like cells, and T cells. Four additional cell types, endothelial, epithelial, interrenal, and mesenchymal cells, were detected in the snRNA-seq dataset, but appeared to be lost during preparation of the single cell suspension submitted for scRNA-seq library generation. We identified additional heterogeneity and subpopulations within the B cells, T cells, and endothelial cells, and revealed developmental trajectories of heamatopoietic stem cells into differentiated granulocyte and mononuclear phagocyte populations. Gene expression profiles of B cell subtypes revealed distinct IgM and IgT-skewed resting B cell lineages and provided insights into the regulation of B cell lymphopoiesis. The analysis revealed eleven T cell sub-populations, displaying a level of T cell heterogeneity in salmon head kidney comparable to that observed in mammals, including distinct subsets of *cd4/cd8*-negative T cells, such as *tcrγ* positive, progenitor-like, and cytotoxic cells. Although snRNA-seq and scRNA-seq were both useful to resolve cell type-specific expression in the Atlantic salmon head kidney, the snRNA-seq pipeline was overall more robust in identifying several cell types and subpopulations. While scRNA-seq displayed higher levels of ribosomal and mitochondrial genes, snRNA-seq captured more transcription factor genes. However, only scRNA-seq-generated data was useful for cell trajectory inference within the myeloid lineage. In conclusion, this study systematically outlines the relative merits of scRNA-seq and snRNA-seq in Atlantic salmon, enhances understanding of teleost immune cell lineages, and provides a comprehensive list of markers for identifying major cell populations in the head kidney with significant immune relevance.

* Corresponding author.
** Corresponding author.
E-mail addresses: daniel.macqueen@roslin.ed.ac.uk (D.J. Macqueen), johanna.hol.fosse@vetinst.no (J.H. Fosse).
[1] equal contribution.

https://doi.org/10.1016/j.fsi.2024.109357
Received 27 October 2023; Received in revised form 19 December 2023; Accepted 21 December 2023
Available online 4 January 2024

1. Introduction

Cells can be classified into distinct types based on their developmental and tissue origin, function, and properties including size, density, and expression of surface markers. Histological examination can only identify a limited range of cell types reliably in tissue sections, and examining specific cell types in their morphological context requires antibodies (for immunostaining) or RNA probes (for *in situ* RNA hybridisation) to robust cell type-specific targets. Furthermore, methods to identify, isolate, and characterise individual cell populations, such as flow cytometry- or magnetic bead-assisted cell sorting, depend on cell type-specific labelling by antibodies to surface molecules or the genetic insertion of lineage-driven fluorescent proteins. An incomplete knowledge of cell-type specific molecules, coupled with the limited availability of specific research reagents for such targets, limits our scope to understand the fundamental biology of many non-model species, such as Atlantic salmon (*Salmo salar*), including in studies of the immune system [1].

One way to overcome such barriers is to harness high-throughput sequencing technologies, which allow biological systems to be investigated without antibodies or pre-selected markers. For many years, RNA sequencing (RNA-Seq) from whole organs or tissues (bulk RNA-seq) has been instrumental to understand transcriptional responses in fish immunology [2]. Despite such advances, bulk RNA-seq measures the average level of gene expression of all cells in a sample, meaning cellular heterogeneity is masked, and key information (such as expression from rare cell types) is lost. The recent rapid development of single cell-resolved omics overcomes this limitation. Single-cell RNA sequencing (scRNA-seq) is the current gold standard for studies of the mammalian transcriptome [3] and has been applied to many non-model animals including fish and shellfish used in aquaculture [4]. The main advantage of scRNA-seq is that each transcript is assigned to a single cell, allowing cell types to be clustered and classified based on similarity in gene expression. In this way, scRNA-seq unveils immune cell heterogeneity, facilitates the discovery of new and rare cell types, and aids the identification of marker genes for specific cell populations [5,6]. Furthermore, marker genes defined by scRNA-seq are potential targets for antibody development and *in situ* hybridisation assays to understand the spatial organisation of cell types within tissues.

An alternative approach to scRNA-seq is to analyze the RNA within nuclei isolated from a tissue. This method, referred to as single nucleus sequencing (snRNA-seq), provides comparable gene detection sensitivity to scRNA-seq, even though the amount of nuclear RNA is lower than that of the whole cell [7]. As snRNA-seq, unlike standard scRNA-seq, is compatible with frozen tissue samples, it has several practical benefits that are particularly suited to the study of aquaculture species [4]. On the other hand, several studies have indicated that scRNA-seq and snRNA-seq differ in their ability to detect certain cell types under specific assay conditions [8,9].

The teleost head kidney contributes to the immune response against microbes as a primary and secondary lymphoid organ and is considered a functional homologue of both the mammalian bone marrow and adrenal gland. Due to its important roles in the immune system, the head kidney has been extensively studied [10,11]. In line with its haematopoietic function, the head kidney is highly heterogeneous and contains diverse cell types that have been identified by scRNA-seq in different species, including three-spined stickleback (*Gasterosteus aculeatus*) [12], broadnosed pipefish (*Syngnathus typhle*) [13], Nile tilapia (*Oreochromis niloticus*) [14,15] and flounder (*Paralichthys olivaceus*) [16].

In this study, we compared the performance of scRNA-seq and snRNA-seq to resolve cellular heterogeneity in the head kidney of healthy farmed Atlantic salmon, where an improved understanding of immune-relevant cell biology has applied value for understanding disease and vaccination outcomes. We deliver a comprehensive list of markers that robustly identifies the major cell populations of head kidney. Our findings reveal that the snRNA-seq is more robust for identifying certain cell types and highlight that protocol-specific biases in the sample preparation pipeline for scRNA-seq may result in loss of entire cell populations. We describe distinct developmental B cell states as well as subpopulations of head kidney T cells and endothelial cells, and reveal distinct developmental trajectories within the myeloid lineage from haematopoietic stem cells. Our findings offer novel insights into the cellular composition of the Atlantic salmon head kidney and reveal extensive differential expression of Atlantic salmon-specific transcription factor paralogues across different cell types and developmental stages. Overall, this study provides an important foundation for further immunological investigations and offers a rich toolbox of marker genes for investigating the role of head kidney cellular heterogeneity in vaccination and infectious disease.

2. Methods

2.1. scRNA-seq sample preparation

Two healthy Atlantic salmon (approximately 180 g body weight) were reared and kept in freshwater at the Center for Sustainable Aquaculture at Norwegian University of Life Sciences (NMBU, Ås, Norway). Fish were maintained on a 24 h light photoperiod in circular tanks in a temperature-controlled recirculation system (14 ± 1 °C) and fed to satiation with a standard commercial diet. Fish were anaesthetized with 300 mg/L tricaine methanesulfonate (MS-222, Argent Chemical Laboratories, WA, USA) and blood was collected by caudal venipuncture for another experiment. Fish were killed by cervical sectioning, and the head kidney was sampled and placed in Leibovitz-15 medium (Lonza Bioscience, catalog no. 12–700F) supplemented with 5 % fetal bovine serum (Avantor, catalog no. 97068-085), 4 mM L-glutamine (Sigma-Aldrich, catalog no. 59202C), and 1 % penicillin/streptomycin/amphotericin (Biowest, catalog no. L0010) and kept on ice.

With a 1 mL syringe plunger, the head kidney tissue was gently passed through a Falcon strainer (70 μm) positioned on a Petri dish containing 5 mL of phosphate-buffered saline (PBS). The Falcon strainer was washed with an additional 5 mL of PBS, and the cell suspension filtered through a 30-μm strainer into a 50 mL Falcon tube. The cell suspension was centrifuged at 500×*g* for 5 min at 10 °C. The resulting pellet was re-suspended and layered onto a discontinuous Percoll gradient with a range of 1.04 and 1.09 g/L. The Falcon tube was centrifuged at 500×*g* for 60 min at 10 °C. The cells at the interface of the Percoll gradient were collected, washed three times in DPBS (Dulbecco's phosphate-buffered saline, Sigma-Aldrich, catalog no. D8537), supplemented with 0.04 % ultrapure bovine serum (BSA, Invitrogen, catalog no. AM2616) then centrifuged at 500×*g* for 5 min at 10 °C. The cells were manually counted using a hemocytometer and re-suspended in DPBS 0.04 % BSA to a final concentration of 900 cells/μL for scRNA-seq library preparation (see below). Both single-cell suspensions showed a viability of 95 %, as evaluated by propidium iodide (0.02 mg/mL) staining and flow cytometry (ACEA Novocyte 3000, Agilent, CA, USA). All the experiments were performed over ice, and the tubes were placed on ice for transportation.

2.2. snRNA-seq sample preparation

Two healthy Atlantic salmon (approximately 25 g body weight) were reared and sampled as previously described [17]. Briefly, the fish were kept in freshwater tanks maintained at 14 °C at the University of Aberdeen (Scotland, UK), and fed to satiation with a commercial salmon diet. Fish were anaesthetized using 2-phenoxyethanol (Sigma–Aldrich, catalog no. 77699) (0.0025 % v/v in water) and given an intraperitoneal injection of PBS (100 μL), before sampling 24 h later after administration of a lethal dose of 2-phenoxyethanol (0.1 % v/v in water) and destruction of the brain. Head kidney samples were flash frozen on dry ice prior to nuclear isolation. Liver and spleen samples of the fish used for snRNA-seq were analysed in separate studies [17] and [18].

Nuclear isolation followed a Tween with salts and Tris buffer (TST) based method adapted from Refs. [17,19]. Briefly, approximately 45 mg flash frozen head kidney tissue per fish was placed in a 6-well tissue culture plate (Stem Cell Technologies, catalog no. 38015) with 1 mL TST buffer (2 mL of 2× ST buffer, 120 μL of 1 % Tween-20 (Sigma-Aldrich, catalog no. P-7949), 20 μL of 2 % BSA (New England Biolabs, catalog no. B9000S), 1.86 mL nuclease-free water) and minced using Noyes spring scissors (Fine Science Tools, catalog no. 15514-12) for 10 min on ice. The homogenate was filtered through a 40-μm cell strainer (Thermo Fisher Scientific, catalog no. 08-771-2), and a further 1 mL of TST was added. To the nuclei suspension, 3 mL of 1× ST solution (diluted from 2× ST buffer [290 μL of 146 mM NaCl (Thermo Fisher Scientific, catalog no. AM9759), 100 μL of 10 mM Tris-HCl pH 7.5 (Thermo Fisher Scientific, catalog no. 15567027), 10 μL of 1 mM CaCl2 (Vwr, E506-100 mL), 210 μL of 21 mM MgCl2 (Sigma–Aldrich, catalog no. M1028), brought up to 10 mL with nuclease-free water]) was added to achieve a final volume of 5 mL. The sample was centrifuged at 500×*g* for 5 min at 4 °C before the resulting pellet was re-suspended in 500 μL of 1× ST buffer and filtered through a 40-μm cell strainer.

2.3. cDNA library preparation and sequencing

The scRNA-seq libraries were prepared at the Genomics Core Facility at Oslo University Hospital (Oslo, Norway) using the Single Cell 3′ Reagent Kit v3.1 from 10× Genomics (Pleasanton, CA) following the manufacturer's protocol. Sequencing of scRNA-seq libraries was done using an Illumina NextSeq500 (San Diego, CA, USA), aiming to recover 6000 cells per library and generating 150 base pair (bp) paired-end reads. The snRNA-seq libraries were processed in the same way at the University of Edinburgh, using head kidney nuclei as input. The scRNA-seq libraries were sequenced on an Illumina NovaSeq 6000 by Novogene UK Ltd, aiming to recover 7000 nuclei per library and generating 150 bp paired-end reads.

2.4. Data analysis

The current Atlantic salmon reference genome (Ssal_v3.1; GCA_905237065.2) was downloaded from Ensembl version 106 (https://www.ensembl.org/Salmo_salar/Info/Index). The mitochondrial assembly and annotations from the previous reference (ICSASG_v2; GCA_000233375.4) were appended to this reference. STARsolo (2.7.10a) [20] was used to map the raw reads (fastq files) for both the scRNA-seq and snRNA-seq datasets to this genome, demultiplex and error correct cell barcodes, and quantify per-cell gene expression. The 'STAR' command was used with the following parameter changes: -outSAMtype BAM SortedByCoordinate, –soloType CB_UMI_Simple, –clipAdapterType CellRanger4, –soloFeatures GeneFull_Ex50pAS, –soloUMIdedup 1 MM_CR, –outFilterMatchNmin 40, –outFilterScoreMin 40, –soloBarcodeReadLength 0, –soloUMIfiltering MultiGeneUMI_CR, –soloCellFilter EmptyDrops_CR, –soloMultiMappers EM. Summary statistics for mapping rates are provided in Supplementary Table 1.

The unfiltered count matrices were then processed by Cellbender (0.3.0) [21], to infer and remove the ambient RNA signal and perform cell calling. Optimal settings for expected cell numbers and total droplets to include were estimated with ranked barcode plots and the number of epochs set to 200. QC was performed separately for each dataset using Seurat (version 4.1.0) [22]. Cells with fewer than 150 genes or unique molecular identifiers (UMIs), or with greater than 20 % of the UMIs associated with mitochondrial genes, were removed from downstream scRNA-seq analysis. Nuclei with fewer than 200 genes or 300 UMIs, or with more than 10 % of UMIs associated with mitochondrial genes were removed from downstream snRNA-seq analysis. Data was normalised using two methods: "lognormalization" with standard Seurat parameters for visualisation purposes and with "SCTransform" for clustering and to generate UMAPs.

Cell annotation was performed by first undertaking a manual exploration of the data using *a priori* markers from other studies in fish and mammals to annotate the broad cell lineages (Supplementary Table 2). These *a priori* markers proved to be of variable specificity thus a list of highly specific markers for each major cell lineage was generated and populations re-annotated by performing high-resolution clustering (resolution of 10 in the "findClusters" Seurat command) and automatically annotating each cluster using the following criteria: mean absolute expression of markers >0.1; at least 40 % of cells expressing all marker genes; and the mean expression greater than 0.5 standard deviations above the mean expression for the dataset. Clusters assigned no identity were manually inspected and assigned. Clusters with two potential identities were identified as potential doublets. If the command "findDoubletClusters" in scDblFinder (1.14.0) [23] also identified these clusters as doublets, they were removed. scDblFinder was also used to identify and remove homotypic doublets (doublets formed from transcriptionally similar cells). The two replicates of each dataset were integrated using Harmony [24] and downstream analysis performed separately for scRNA-seq and snRNA-seq. Individual analysis and clustering of subpopulations (T cell, B cell, endothelial, and myeloid lineages) was performed by creating separate Seurat objects, normalising with sctransform, and clustering with Seurat before manual identification of each population.

For the analysis comparing the expression levels of transcription factor genes between scRNA-seq and snRNA-seq datasets, we obtained a list of 931 genes from the Atlantic salmon genome (Ssal_v3.1) annotated with the gene ontology (GO) term "*DNA-binding transcription factor activity*" (GO:0003700) using Biomart [25]. We then used this list to calculate the percentage of UMIs mapped to candidate transcription factor genes in both the scRNA-seq and snRNA-seq datasets. This analysis was only performed on cell populations present in both datasets.

PHATE [26] was used to perform trajectory analysis on particular populations identified within the scRNA-seq and snRNA-seq datasets. Seurat objects were generated to combine the haematopoietic stem cells cluster with the granulocyte and mononuclear phagocyte clusters in turn. The count matrix was renormalised with sctransform and the phateR (v1.0.7) package used to calculate 2-dimensional PHATE embeddings from the sctransform generated residuals. Clustering based on the PHATE embeddings was performed using the FindNeighbors and FindClusters Seurat functions.

Gene annotations were taken from the Ensembl annotation for Atlantic salmon. For genes with no name, Biomart [25] was used to identify orthologues in other species (all salmonids, northern pike, zebrafish, medaka, chicken, mouse and human) and the gene name from the most closely related gene was used. Biomart was also used to find predicted protein products in support of annotation.

For visualisation of the relationship between cell clusters from each dataset, we performed differential genes expression tests for all clusters and plotted a Sankey diagram using the R package networkD3 (https://cran.r-project.org/web/packages/networkD3/index.html) to visualise the number of shared marker genes between populations in the scRNA-seq and snRNA-seq data. Pearson rank correlation values between clusters were calculated based on the average expression of all marker gene in each cluster.

3. Results

scRNA-seq and snRNA-seq datasets were generated from head kidneys of healthy Atlantic salmon from independent samplings and stocks (two animals per method), using shared parameters for mapping, annotation, and quality control. The two datasets were analysed in parallel rather than integrated to ensure unbiased (i.e. independent) inferences on their performance in capturing cellular heterogeneity and cell-specific marker genes. It is important to note that the difference in fish size between the two experiments presents a potential limitation that may affect the direct comparison of cell type composition, with

scRNA-seq conducted on fish weighting 180 g and snRNA-seq on fish weighting 25 g.

3.1. snRNA-seq identified more unique head kidney cell types

14,149 cells and 18,067 nuclei passed filtering and were used for downstream analysis. The full list of marker genes for each cluster is provided in Supplementary Table 3.

Eight major cell populations were identified in both datasets: granulocytes, haematopoietic stem cells (HSC), erythrocytes, mononuclear phagocytes (MP), thrombocytes, B cells, natural killer-like (NK-like) cells, and T cells. Four additional clusters were identified in the snRNA-seq dataset only: endothelial cells, mesenchymal cells, a small population of interrenal cells, and a cluster of epithelial cells (Fig. 1A). Screening endothelial marker transcripts at the sequential steps of sample preparation revealed that endothelial cells were lost during filtering of the single cell suspension prior to library preparation, suggesting incomplete vascular stalk dissociation (Supplementary Fig. 1). The percentage of cells in most cell clusters were higher in snRNA-seq, except for granulocytes, which represented more than half of the cells recovered by scRNA-seq (Fig. 1B). Supplementary Fig. 2 displays the percentage of cell populations in each fish for each of the analyses.

Fig. 1C shows the proportion of marker genes either shared between the two datasets or unique to scRNA-seq or snRNA-seq, respectively. The number of unique markers was generally higher in the snRNA-seq dataset. Cluster-specific markers identified in each dataset were compared by Pearson correlation coefficient analysis. Despite the lack of formal dataset integration, markers of most cell types correlated well between datasets (Fig. 1D). In line with previous studies, a much higher proportion of reads in the scRNA-seq dataset mapped to genes encoding mitochondrial or ribosomal proteins, while a higher proportion of reads in the snRNA-seq dataset mapped to genes encoding transcription factors (Supplementary Figs. 3–4). The expression of ribosomal genes was particularly high in HSC and MPs identified by scRNA-seq, likely contributing to the low number of shared markers in these cell populations (Fig. 1C). Correspondingly, the ribosomal gene content of thrombocytes and NK cells was relatively low, and these cell types showed a high number of shared markers between the two datasets.

3.2. Identification of robust marker genes for cell type annotation

Our analysis generated a set of robust cell type-identifier genes that consistently assigned each cell cluster to a specific lineage using both scRNA-seq and snRNA-seq (Fig. 2B, Supplementary Table 2). All cell type-identifier genes were expressed and allowed the annotation of cell clusters in both datasets, despite some variation in expression level. Ensembl gene IDs are included in the text and supplementary tables to distinguish the numerous paralogues retained from sequential whole genome duplication events in the teleost and salmonid ancestors [27–29]. Marker genes for cell clusters that were exclusively present in either the scRNA-seq or snRNA-seq dataset are indicated within the text using ‘sc-only’ or ‘sn-only’, respectively. Examination of genes with previously described cell type-specificity, some of which were included as cell type-identifiers, followed the expected expression pattern and confirmed the identity of the cell clusters (Fig. 2C).

3.3. Atlantic salmon head kidney cell populations recovered in both datasets

3.3.1. B cells

Similar numbers and relative proportions of B cells were identified in both datasets, with 4211 (30 % of total cells) recovered by scRNA-seq and 5293 (29 % of total) by snRNA-seq. The B cell cluster showed high expression of well-characterised B cell markers, including *swap70* (ENSSSAG00000115076, ENSSSAG00000118232), *cd79a* (ENSSSAG00000113980), *ebf1* (ENSSSAG00000041858, ENSSSAG00000070298, ENSSSAG00000079780), *pax5* (ENSSSAG00000104911), and several immunoglobulin-related genes. Interestingly, certain classic pan B cell markers, like *cd79a* and *cd22* (ENSSSAG00000001154 [sc-only]), were highly expressed not only by B cells, but also by other Atlantic salmon head kidney cell populations. Specifically, one T cell subcluster expressed *cd79a*, whereas granulocytes and erythrocytes expressed different paralogues of *cd22* (ENSSSAG00000001154, ENSSSAG00000053845, respectively). Nevertheless, combining *cd79a* with a set of other markers, including *cd37* (ENSSSAG00000065541), *bcl11aa/ab* (ENSSSAG00000074341 [sn-only], ENSSSAG00000078113, ENSSSAG00000086930, ENSSSAG00000119971), and *pax5* (ENSSSAG00000104911) reliably identified Atlantic salmon B cell populations in both datasets. Subpopulations of B cells are described in section 3.5.1.

3.3.2. T cells

Unlike B cells, the recovery of T cells differed markedly between datasets. Only 467 T cells (3 % of total cells) were recovered by scRNA-seq, while snRNA-seq recovered 3057 (17 % of total), representing a six-fold increase. The influence of fish size on the proportional abundance of immune cells across various tissues and organs remains unclear. Nonetheless, several studies report a downregulation of immune genes associated with smoltification induced by adjustments in photoperiod and seawater acclimatization [30–32]. Although none of the fish used in the current study were exposed to altered light periods or seawater conditions, the large size of the fish used for scRNA-seq makes it likely that they would have undergone at least some of these smoltification-induced changes in the immune system, which are still poorly understood.

Among the genes used to identify T cells were *cd3e* (ENSSSAG00000076824), *cd28* (ENSSSAG00000083857), *tcf7* (ENSSSAG00000006857, ENSSSAG00000064204), *bcl11b* (ENSSSAG00000045088, ENSSSAG00000071984), *ly9* (ENSSSAG00000040550), and *prkd3* (ENSSSAG00000068132, ENSSSAG00000075988). Subpopulations of T cells are described in section 3.5.2.

3.3.3. Erythrocytes

Erythrocytes were recovered from both datasets with 151 (1 % of total cells) identified by scRNA-seq and 957 (5 % of total) by snRNA-seq. The low number of erythrocytes retrieved by scRNA-seq was expected, considering the density gradient centrifugation before library preparation. The erythrocytes formed a well-defined population with high expression of haemoglobin genes including *hba/aa2* (ENSSSAG00000044737, ENSSSAG00000095264, ENSSSAG00000065229, ENSSSAG00000086616), *hbb1* (ENSSSAG00000045065), *hbe1* (ENSSSAG00000048536, ENSSSAG00000065233) and *hbba2* (ENSSSAG00000111938, ENSSSAG00000088798, ENSSSAG00000103747). Other highly expressed genes in this cluster were *alas2* (ENSSSAG00000068428), *ank1/a* (ENSSSAG00000078696, ENSSSAG00000047949) and *cahz* (ENSSSAG00000085097).

3.3.4. Granulocytes

The granulocyte cluster was the only cluster with a higher proportion of cells identified using scRNA-seq, comprising 7268 cells (51 % of total), compared to 2522 (14 % of total) for snRNA-seq. This cluster was enriched for genes encoding oxidative, proteolytic and glycolytic enzymes including *mpx* (ENSSSAG00000000157, ENSSSAG00000048994), *mmp9* (ENSSSAG00000042609 [sc-only], ENSSSAG00000069874), *mmp13* (ENSSSAG00000070495), *f264* (ENSSSAG00000081699), *gpi* (ENSSSAG00000055699), and *g6pd* (ENSSSAG00000068731). One of the most highly expressed genes in this cluster encodes nephrosin (*npsn* - ENSSSAG00000079745), a zinc metalloendopeptidase expressed by zebrafish granulocytes that contributes to defence against bacterial infections [33].

3.3.5. Haematopoietic stem cells

A cluster of cells expressing genes including *cdk6*

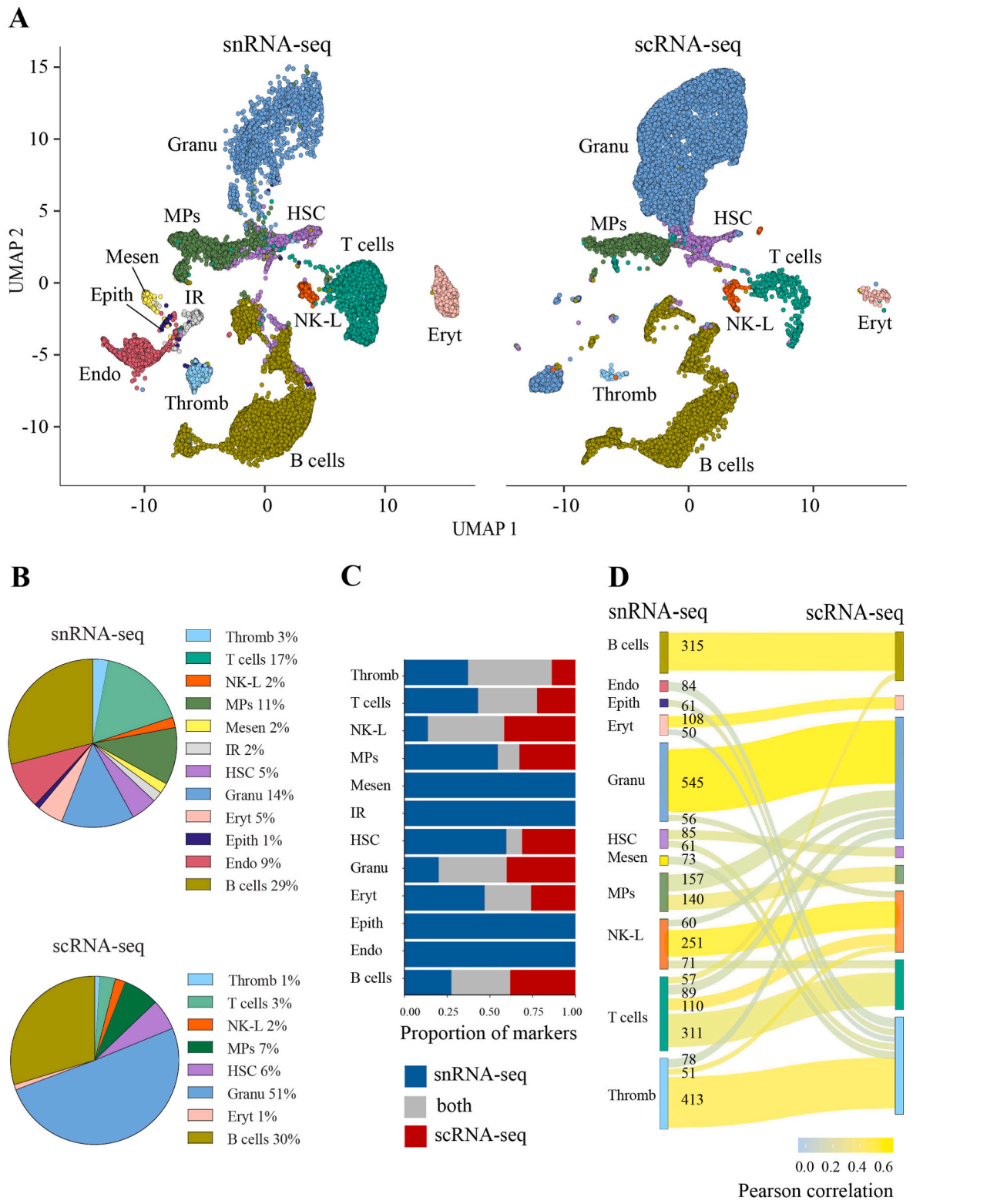

Fig. 1. *Comparison of snRNA-seq and scRNA-seq annotations of head kidney cellular heterogeneity in Atlantic salmon.* (A) UMAP (Uniform Manifold Approximation and Projection) of cell types identified by sc/snRNA-seq. Each cluster is coloured by cell type. (B) Pie charts showing the proportions of each cell type from scRNA-seq and snRNA-seq. (C) Proportion of cell population markers unique to or shared by scRNA-seq and snRNA-seq. (D) Sankey network plot showing the correlation of marker genes for each cell population between datasets. The width of lines linking common cell clusters corresponds to the number of shared markers. The line colours reflect Pearson correlation scores between datasets following the scale provided. The number of common markers is displayed. Clusters that do not appear on the plot have less than 50 shared marker genes. Endo – endothelial cells, Epith – epithelial cells, Eryt – erythrocytes, Granu – granulocytes, HSCs – haematopoietic stem cells, IR – interrenal cells, Mesen – mesenchymal cells, MPs – mononuclear phagocytes, NK-L – natural killer-like cells and Thromb – thrombocytes.

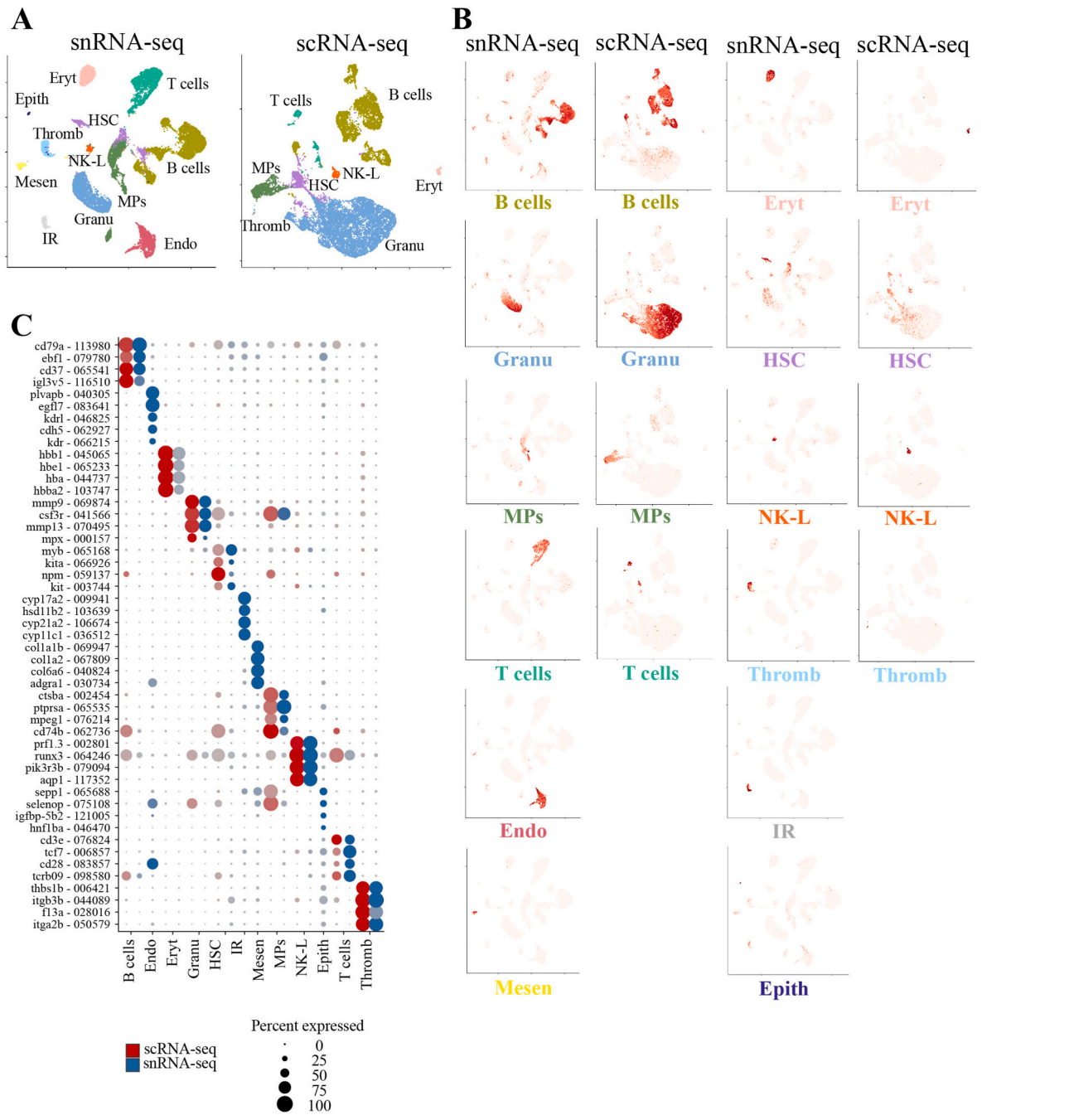

Fig. 2. *Selected cell type-identifier genes for each population.* (A) UMAP of cell types identified by scRNA-seq and snRNA-seq. Each cluster is coloured by cell type. (B) Feature plots showing the distribution of cell type-identifier genes (Supplementary Table 2) in each Atlantic salmon head kidney cell population in scRNA-seq and snRNA-seq datasets, respectively. (C) The expression of genes with previously described cell type-specificity (Supplementary Table 4) in each cell population. Red and blue dots show markers for scRNA and snRNA data, respectively. The intensity of the dot colours corresponds to the level of expression, with darker shades indicating higher expression levels and lighter shades indicating lower expression levels. The dot sizes corresponds the percentage of cells/nuclei in the cluster that express the gene. The number next to the gene name provides the last six digits of the Ensembl accession number.

(ENSSSAG00000100175), *egr1* (ENSSSAG00000093647 [sc-only]), *kit/a* (ENSSSAG00000003744, ENSSSAG00000066926), *tisb* (ENSSSAG00000005642) and *npm/1a* (ENSSSAG00000059137, ENSSSAG00000005676) was classified as HSCs, featuring 811 cells (6 % of total) in the scRNA-seq dataset and 892 cells (5 % of total) in the snRNA-seq dataset.

3.3.6. *Mononuclear phagocytes*

Neither global cell clustering nor attempts at subclustering allowed a clear distinction between head kidney macrophages, monocytes, and dendritic cells in any of the two datasets, in contrast to another article published in this special issue describing MP heterogeneity in Atlantic salmon spleen [18]. Instead, these cells formed a common cluster. The cluster was identified in both datasets, with fewer cells recovered by scRNA-seq (955 cells, 7 % of all cells) than snRNA-seq (1984 cells, 11 % of all cells). MPs expressed classical markers of antigen presenting cells, such as *mpeg1* (ENSSSAG00000076214), *csfr1/a* (ENSSSAG00000061479, ENSSSAG00000001705, ENSSSAG00000005676) and *cd74/b* (ENSSSAG00000004635, ENSSSAG00000062736).

3.3.7. NK-like cells

NK-like cells were identified by the expression of genes including *prf1* (ENSSSAG00000002801, ENSSSAG00000009129), *runx3* (ENSSSAG00000064246), *aqp1* (ENSSSAG00000117352), *mafa/*b (ENSSSAG00000108168, ENSSSAG00000052644, ENSSSAG00000008494 [sc-only], ENSSSAG00000113089 [sc-only] and *arid3c* (ENSSSAG00000043118), consistent with the NK-like cell cluster described previously in Atlantic salmon liver [17]. The NK-like cluster was relatively small, comprising only 219 cells (<2 % of total) in the scRNA-seq dataset and 284 cells (<2 % of total) in the snRNA-seq dataset. The highest expressed NK-like marker was *pik3r3b* (ENSSSAG00000079094), which encodes a regulatory subunit of class 1 phosphoinositide 3-kinases crucial for the effector function of mammalian NK cells [34].

3.3.8. Thrombocytes

Thrombocytes were identified in both datasets. While scRNA-seq only identified 67 thrombocytes (<1 % of total cells), snRNA-seq recovered 612 (3 % of total cells). The cluster was defined by classical thrombocyte markers, such as *thbs1b* (ENSSSAG00000006421), *itgb3b* (ENSSSAG00000044089), *f13a* (ENSSSAG00000028016), *itga2b* (ENSSSAG00000050579, ENSSSAG00000051488), and *mpl* (ENSSSAG00000045689, ENSSSAG00000079193), but also *gata1* (ENSSSAG00000008520, ENSSSAG00000081386), and *lmo2* (ENSSSAG00000052180).

3.4. Atlantic salmon head kidney cell populations recovered by snRNA-seq only

Four clusters of cells were only identified by snRNA-seq. For this section, all Ensembl IDs originate from the snRNA-seq dataset.

3.4.1. Endothelial cells

The endothelial cell cluster contained 1601 cells (9 % of total). These cells showed enrichment of several homologues of well-characterised endothelial-specific genes including *egfl7* (ENSSSAG00000083641), *tek* (ENSSSAG00000096369, ENSSSAG00000072071) (alias *tie2*), *robo4* (ENSSSAG00000051277), and *cdh5* (ENSSSAG00000062927) (alias *VE-cadherin*). The cluster also showed highly specific expression of homologues of zebrafish-identified endothelial marker genes, including *kdrl* (ENSSSAG00000046825, ENSSSAG00000054371) and *dusp5* (ENSSSAG00000027885, ENSSSAG00000007089). Endothelial cell subpopulations are described in section 3.5.3.

3.4.2. Interrenal cells

Another cluster was designated interrenal cells and contained 419 cells (2 % of total). Its identification was based on the expression of mitochondrial cytochrome P450 (cyp) enzymes, including *cyp11b* (ENSSSAG00000086140), *cyp17a2* (ENSSSAG00000009941), *cyp21a2* (ENSSSAG00000004083, ENSSSAG00000106674) and *cyp11c1* (ENSSSAG00000036512), involved in steroid hormone biosynthesis and production of cortisol in interrenal cells of head kidney [35,36]. The interrenal cell cluster also showed expression of *fdx1b* (ENSSSAG00000070653), in agreement with findings in zebrafish [37] and *nr5a1* (alias *ff1b*) shown to be the first molecular marker for interrenal cells in zebrafish [38].

3.4.3. Mesenchymal cells

Mesenchymal cells represented another small cluster exclusive to snRNA-seq (289 cells, <2 % of total). Cells in this cluster showed fibroblast features, for instance the expression of collagen genes, including *col1a2* (ENSSSAG00000046988, ENSSSAG00000067809), *col6a6* (ENSSSAG00000040824), *col1a1b* (ENSSSAG00000069947), and *col12a1b* (ENSSSAG00000070858), similar to mesenchymal cells of zebrafish and Atlantic salmon liver [17,39]. Cadherins such as n-cadherin (*cdh2* - ENSSSAG00000000678, ENSSSAG00000049983), a mesenchymal cell marker involved in the epithelial-mesenchymal transition [40], and the chemokine *cxcl12* (ENSSSAG00000117767) were also highly expressed in this population.

3.4.4. Epithelial cells

The last of the four cell populations exclusive to the snRNA-seq dataset was a small cluster comprising 157 cells (<1 % of total). These were most likely epithelial cells, on the basis of high expression of *sepp1* (ENSSSAG00000075108, ENSSSAG00000065688), *lrp2a* (ENSSSAG00000081532), *hnf1ba* (ENSSSAG00000046470) and *dab2* (ENSSSAG00000056184), all expressed in epithelial cells of zebrafish kidney [41–43], as well as many genes encoding members of the solute carrier family.

3.5. Subclustering reveals distinct cellular subsets

Following the primary global clustering, we investigated B cells, T cells, and endothelial cells in more detail using subclustering analyses. For this, we extracted the cells belonging to the cluster of interest and conducted a new clustering to the exclusion of other cell types, aiming to identify different subpopulations and associated marker genes within each targeted cell type.

3.5.1. Identification of head kidney B cell subpopulations at distinct developmental stages

Comparable numbers and proportions of B cells were identified in the scRNA-seq and snRNA-seq datasets. The head kidney is the main site of B cell lymphopoiesis in teleost fish, and previous work in rainbow trout demonstrated the presence of different developmental B cell stages in the salmonid head kidney [44,45]. We performed separate subclustering of the global B cell clusters identified by snRNA-seq and scRNA-seq, again without integration. Both analyses identified five B cell subclusters (Fig. 3A) with overall highly correlated marker genes (Fig. 3B). Examples of markers for each of the B cell subclusters are shown in Fig. 3C, with the full list of markers in Supplementary Table 5.

In B1, snRNA-seq recovered three times more cells (900 cells, 17 % of all B cells) than scRNA-seq (262 cells, 6 % of all B cells). B1 showed markers characteristic of early B cell development (pro- and early pre-B cells) [44], with upregulation of *ebf1* (ENSSSAG00000070298) and genes involved in V(D)J-rearrangement (*rag1* - ENSSSAG00000004550, *rag2* - ENSSSAG00000004544 [sc-only], *sox4* - ENSSSAG00000112690, ENSSSAG00000099132, ENSSSAG00000105188 [sn-only], *dntt* - ENSSSAG00000024940, ENSSSAG00000065644, and *foxo1* - ENSSSAG00000054669)) [46,47]. High expression of *tcf4* (ENSSSAG00000071044, ENSSSAG00000113835), *gfi1ab* (ENSSSAG00000038567, ENSSSAG00000009977) [48], and *bcl11aa* (ENSSSAG00000078113) was also observed. Compared to the other four B cell clusters, B1 showed low levels of *cd74* (ENSSSAG00000004635), *cd53* (ENSSSAG00000008396 [sn-only], ENSSSAG00000071444), and *cd37* (ENSSSAG00000065541) [49,50].

B2 shared some marker genes with clusters B1 and B3, including *foxo1* (ENSSSAG00000054669) and *cxcr4* (ENSSSAG00000053084, ENSSSAG00000063084, ENSSSAG00000118192 [sc-only]), which is enriched in pre-pro B cells, pro-B cells and pre-B cells [51]. Similar numbers of B2 cells were retrieved from each dataset (755 cells, 18 % of all B cells for scRNA-seq, 830 cells, 16 % of all B cells for snRNA-seq). While *rag1* (ENSSSAG00000070298) was not a marker of B2, the expression of *rag2* (ENSSSAG00000004544 [sc-only]) was further increased compared to B1. Moreover, the transcription factor Ikaros (*ikzf1*, ENSSSAG00000053329 [sn-only]) was enriched in B2, in line with its role in driving the pre-B cell transition [52]. The B2 transcription profile is consistent with proliferating pre-B cells [53], as many of the marker genes encode proteins involved in cell cycle regulation, such as *mki67* (ENSSSAG00000066170), *ptma* (ENSSSAG00000105782 [sc-only], ENSSSAG00000075676 [sc-only]), *ccnd2a2* (ENSSSAG00000095730 [sc-only], ENSSSAG00000016373), gadd45

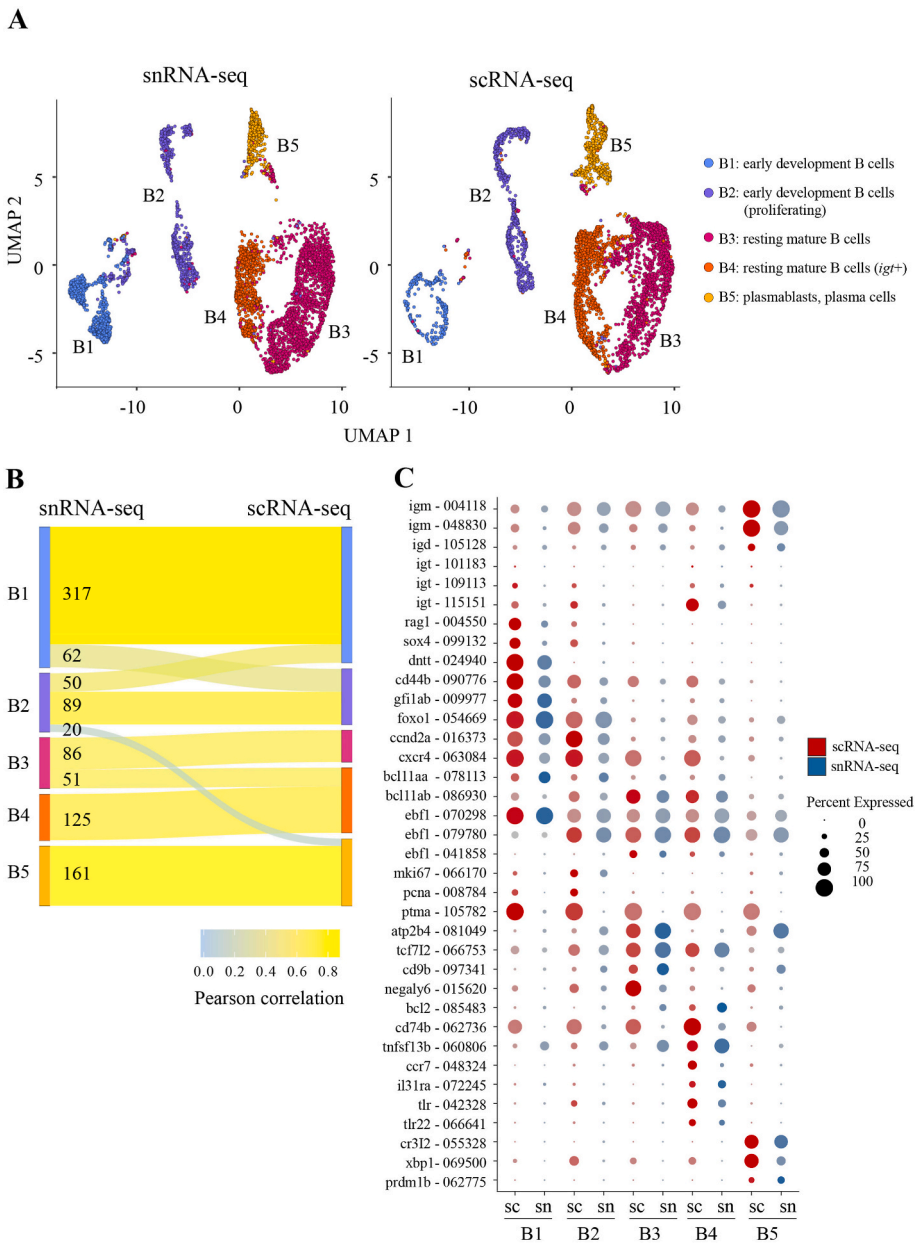

Fig. 3. *Comparison of B cell subtypes identified by scRNA-seq and snRNA-seq.* (A) UMAP of B cell subclusters identified by sc/snRNA-seq. (B) Sankey network plot showing the correlation of marker genes for each B cell subcluster between datasets. The width of the lines linking the sets of clusters corresponds to the number of common markers. The line colours reflect Pearson correlation according to the provided scale. Number of common markers are displayed. (C) Dotplot displaying markers for each B cell subcluster from scRNA-seq and snRNA-seq. The intensity of the dot colour corresponds to the level of expression, with darker shades indicating higher expression levels and lighter shades indicating lower expression levels. The dot sizes corresponds the percentage of cells expressing the gene in each subcluster. The number next to the gene name provides the last six digits of the Ensembl accession number. As highlighted in section 3.3.2 regarding T cells, it is important to consider the difference in size of the fish used for scRNA-seq and snRNA-seq, which could contribute to the observed variations in cell population recovery between the two protocols.

(ENSSSAG00000065713), *pcna* (ENSSSAG00000061142 [sc-only], ENSSSAG00000008784 [sc-only]) and *top2a* (ENSSSAG00000066721). Furthermore, expression of the immunoglobulin light chain-encoding *igl3v5* (ENSSSAG00000116510) started to increase in B2 and was further increased in B3 and B4, but was only a marker of B5.

B3 and B4 displayed profiles consistent with two distinct subsets of resting mature B cells [44,49,54–56]. B3 was the largest identified B cell cluster in both analyses, consisting of 1632 cells (40 % of all B cells) in the scRNA-seq dataset and 2396 (45 % of all B cells) in the snRNA-seq dataset. Both datasets also identified similar proportions of cells in B4, with 801 cells (15 % of all B cells) from scRNA-seq and 1012 (25 % of all B cells) from snRNA-seq.

Both B3 and B4 showed low expression of *rag1* and *rag2* and were enriched for different paralogues of *klf2* (B3: ENSSSAG00000006501, ENSSSAG00000072786, ENSSSAG00000064886; B4: ENSSSAG00000049310), *s1pr4* (B3: ENSSSAG00000069985, B4: ENSSSAG00000119257), *dnmt3a/b* (B3: ENSSSAG00000042714 [sn-only], ENSSSAG00000071787 [sn-only]; B4: ENSSSAG00000071787 [sc-only]) [57], and *baff/tnfsf13b* (B3: ENSSSAG00000054719; B4: ENSSSAG00000060806) [58].

Interestingly, the subclusters appeared to represent two different B cell lineages, based on differential expression of immunoglobulin heavy chains. As the current Ensembl annotation of the Atlantic salmon genome does not include genes encoding immunoglobulin heavy chains,

we conducted BLAST protein searches on some non-annotated genes and assigned names based on sequence homology. We identified three immunoglobulin classes: IgM (ENSSSAG00000004118 and ENSSSAG00000048830) with matches to ACN10898 and ACN10415; IgD (ENSSSAG00000105128) with a match to XP_045575991, and IgT (ENSSSAG00000115151, ENSSSAG00000109113 and ENSSSAG00000101183) with matches to ADD59873, ACX50292 and ACX50293. While IgT (ENSSSAG00000115151) was strongly enriched in B4, the expression of IgM (ENSSSAG00000048830, ENSSSAG00000004118) was higher in B3 than in B4 (although still much lower than in B5), consistent with the concept that B cells become committed to either IgT or IgM lineages during development [59]. The expression of IgD (ENSSSAG00000105128) was comparable in B3 and B4, but only a marker in B5.

In addition, B3 was enriched for *cd37* (ENSSSAG00000065541), *igl3v2* (ENSSSAG00000042545), *ikzf1* (ENSSSAG00000008390 [sn-only]), *ebf1* (ENSSSAG00000041858, ENSSSAG00000079780 [sn-only]) [44,60], *bcl11ab* (ENSSSAG00000086930, ENSSSAG00000119971 [sn-only]) [61], and *cd9b* (ENSSSAG00000097341). On the other hand, B4 showed enrichment for *cd74* (ENSSSAG00000004635, ENSSSAG00000062736), *bcl-2* (ENSSSAG00000085483), *pax5* (ENSSSAG00000104911 [sc-only]), and *ccr7* (ENSSSAG00000048324 [sc-only]).B5 was the most distinct subcluster, with an expression profile consistent with the final stages of B cell differentiation. B5 consisted of 455 cells in the scRNA-seq dataset (11 % of all B cells) and 366 (7 % of all B cells) in the snRNA-seq dataset. During

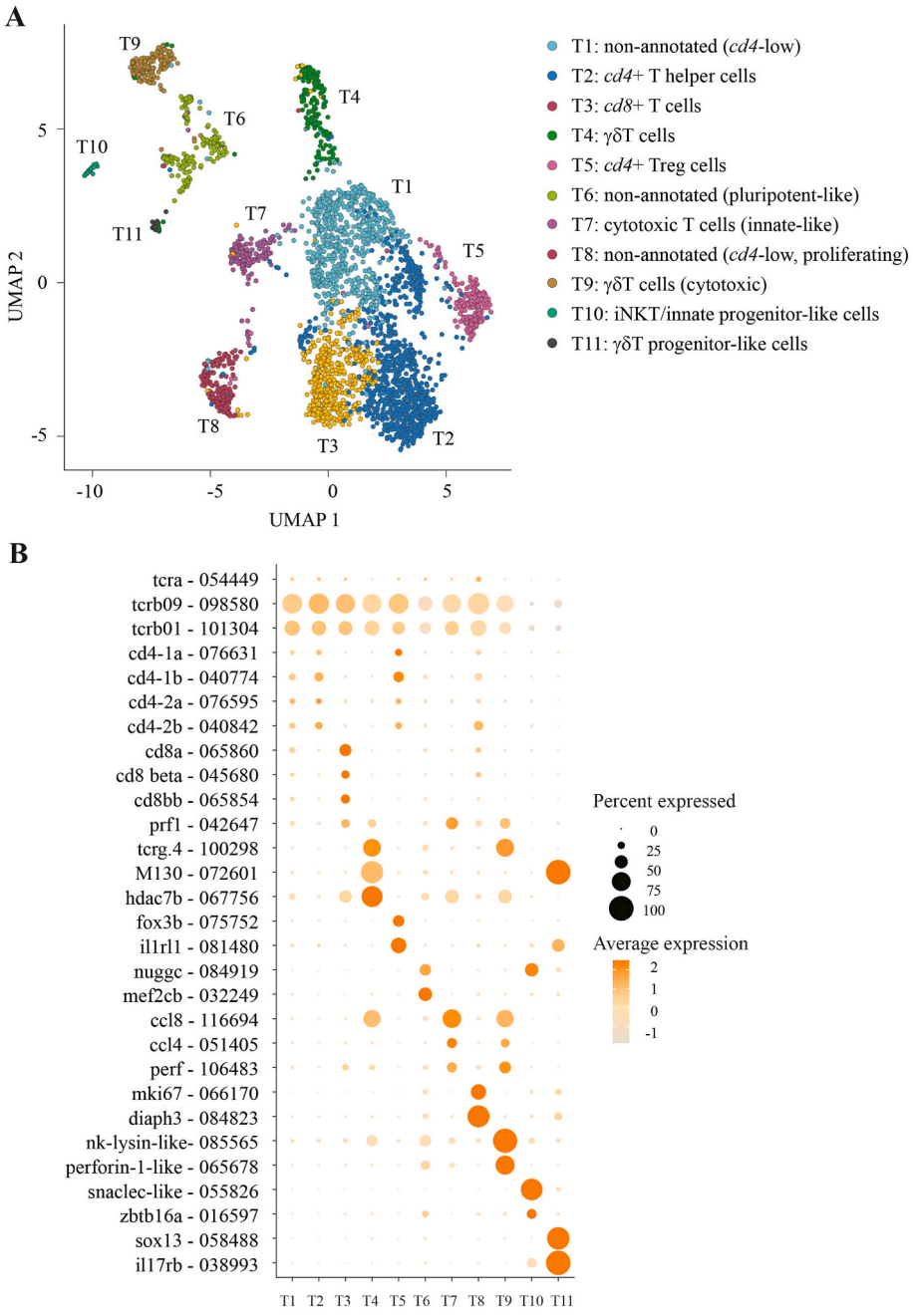

Fig. 4. *Subclustering of the head kidney T cell population.* Due to the limited number of T cells recovered by scRNA-seq, we only show T cell populations from snRNA-seq. Data from scRNA-seq is provided in Supplementary Fig. 5 (A) UMAP of T cell subclusters identified by snRNA-seq. (B) Dotplot displaying markers for each T cell subcluster. The dot colours indicate the average normalised expression of the gene, while dot sizes corresponds the percentage of cells expressing the gene in each subcluster. The number next to the gene name provides the last six digits of the Ensembl accession number.

the transition from plasmablast to plasma cell, *pax5* is downregulated, in parallel to upregulation of transcription factors driving plasma cell development, including *irf4*, *xbp1* and *prdm1* [62,63]. B5 expressed plasmablast and plasma cell markers including *cr3l2* (ENSSSAG00000055328), *xbp1* (ENSSSAG00000071607, ENSSSAG00000069500), *pax5* (ENSSSAG00000104911 [sc-only]), *prdm1* (ENSSSAG00000062775, ENSSSAG00000120858 [sc-only]), and several immunoglobulin-related genes. Hence, this cluster appeared to contain a mixture of plasmablasts and plasma cells in both datasets.

3.5.2. The head kidney contains a diverse range of T cells

Due to the small number of T cells recovered by scRNA-seq, we considered the snRNA-seq dataset most suitable for investigating T cell diversity. Subclustering of the 3057 T cells within the snRNA-seq dataset revealed eleven potential T cell subsets (Fig. 4A), consistent with the notion that Atlantic salmon T cells, like mammalian T cells, take advantage of the haematopoietic niche for long term persistence and maintenance [64]. Fig. 4B and Supplementary Table 6 present marker genes in each T cell subcluster. Supplementary Fig. 5 shows a preliminary subclustering of T cells from scRNA-seq, along with its correlation with snRNA-seq T cell subclusters. All Ensembl IDs referred to in the text derive from the snRNA-seq dataset.

T cells expressing *cd4* were predominantly identified in T2 (876 cells, 29 % of all T cells) and T5 (194 cells, 6 % of all T cells). Atlantic salmon possesses two copies each for *cd4-1* and *cd4-2*. Approximately 28 % of the cells in T2 and T5 co-expressed the teleost *cd4* genes: *cd4-1a and/or cd4-1b* as well as *cd4-2b* (ENSSSAG00000076631, ENSSSAG00000040774, ENSSSAG00000040842), representing a T cell subtype referred to as double positive cd4 T cells [65]. Moreover, in both clusters, around 20 % of cells expressed *cd4-2*, but not *cd4-1*, consistent with a *cd4-2*$^{+}$*cd4-1*$^{-}$ lymphocyte subpopulation described as less proliferative, but still responsive to bacterial infection [65]. Cells in T2 are likely to represent T helper cells, with high expression of molecules involved in T cell receptor recycling and naïve T cell activation, including *ctsl.1* (ENSSSAG00000002302), *prkca* (ENSSSAG00000007052, ENSSSAG00000083362), and *cd28* (ENSSSAG00000083857, ENSSSAG00000007664) [66–68]. Furthermore, the cluster showed enrichment for *s1pr4* (ENSSSAG00000119257), suggesting that at least a proportion of cells are primed to enter the circulation [69]. In contrast, T5 expressed a T regulatory (Treg) signature, including upregulation of *foxp3* (ENSSSAG00000059169, ENSSSAG00000075752), *ikzf4* (ENSSSAG00000096085) and *ikzf2* (ENSSSAG00000058344, ENSSSAG00000110212) [70]. *Foxp1b* (ENSSSAG00000077820) was another marker of the T5 cluster, consistent with its role in the regulation of Treg homeostasis and the expression of *ctla4* (ENSSSAG00000093109) [71].

The T1 and T8 subclusters also expressed low levels of *cd4* transcripts, although not as markers. The large T1 subcluster (682 cells, 22 %) was difficult to identify further. The shared expression of most genes between T cell subsets is a common obstacle when trying to distinguish between them, and the poor annotation and low specificity of many T1 marker genes made it challenging to characterise this cluster. Cells in T8 (156 cells, 5 % of all T cells) expressed many genes involved in cell cycle activation, including *diaph3* (ENSSSAG00000091681, ENSSSAG00000084823), *cenpp* (ENSSSAG00000087528), *kif23* (ENSSSAG00000044381, ENSSSAG00000120697), and *mki67* (ENSSSAG00000066170). Moreover, T8 was enriched for *cd9* (ENSSSAG00000079939), *cxcr4* (ENSSSAG00000053084, ENSSSAG00000063084) and expressed the chemokine receptor *ccr7* (ENSSSAG00000048324).

Cells in subcluster T3 (409 cells, 13 %) represented cytotoxic *cd8*$^{+}$ T cells, based on enrichment for all *cd8* genes annotated in the current Atlantic salmon genome: *cd8b* (ENSSSAG00000045680), *cd8bb* (ENSSSAG00000065854), and *cd8a* (ENSSSAG00000065860). Among the other T3 markers were two perforin-encoding genes (ENSSSAG00000042647, ENSSSAG00000106483), *cxcr3* (ENSSSAG00000115800), and *itga4* (ENSSSAG00000064161), all shown to be expressed by rainbow trout cd8^{+} T cells [72,73].

Two T cell subclusters, T4 (197 cells, 6 % of all T cells) and T9 (153 cells, 5 % of all T cells), appear to have captured distinct γδT cell subtypes. Both expressed one of the five T cell gamma receptor constant genes (*tcrγ*, ENSSSAG00000100298) [74]. T9 may represent activated γδT cells, with markers including three granulysin-encoding genes (ENSSSAG00000003357, ENSSSAG00000085565, ENSSSAG00000009411), three perforin-encoding genes (ENSSSAG00000106483, ENSSSAG00000065678, ENSSSAG00000005439) [75], and *id3* (ENSSSAG00000107585). T4 did not express any of these markers, but expressed other cytotoxic genes at lower levels, suggestive of a functionally distinct or dormant γδT cell population.

While cluster T11 (33 cells, 1 % of all T cells) did not express *tcrγ*, it expressed other genes typical of mammalian γδT cells, including *sox13* (ENSSSAG00000077869, ENSSSAG00000058488), *il17rb* (ENSSSAG00000038993), and *il21rb* (ENSSSAG00000041003, ENSSSAG00000055593) [76], possibly representing prothymic γδT cell progenitors [77]. Enrichment for *gata2* (ENSSSAG00000079702, ENSSSAG00000068560) and *gata3* (ENSSSAG00000044928, ENSSSAG00000065097) were in line with the assumed progenitor nature of this subset [78,79]. However, enrichment for *il17rb*, *gata2*, *gata3*, and *il1rl1* (ENSSSAG00000081478, ENSSSAG00000081480) is also seen in innate lymphoid cell progenitors [80]. T11 was also enriched for ENSSSAG00000072601, encoding the scavenger receptor M130, a marker shared with T4. This is interesting, as two T cell subsets with dual expression of *tcrγ* and M130 (similar to T4) or gata3 and M130 (similar to T11) were recently described in Atlantic cod (*Gadus morhua*) spleen [81].

The majority of cells in T6 (165 cells, 5 %) and T7 (159 cells, 5 %) were double negative for *cd4* and *cd8* (*cd4*$^{-}$*cd8*$^{-}$) [82]. Based on expression of cytotoxic mediator genes encoding granulysins (ENSSSAG00000052253, ENSSSAG00000010873), perforins (ENSSSAG00000042647, ENSSSAG00000106483, ENSSSAG00000006878), and granzyme (ENSSSAG00000052253), these cells could represent different cytotoxic T cell populations with properties resembling those of mammalian CD3^{+}CD4^{-}CD8^{-} double-negative cytotoxic T cells [83]. This hypothesis was supported by high expression of ENSSSAG00000092386, elsewhere annotated as *fcer1gl* (NCBI Gene ID: 106569423), which in mouse and human markers an innate-like T cell population with high cytotoxic potential [84]. Other markers of T7 included *ccl8* (ENSSSAG00000116694), *il2rb* (ENSSSAG00000050463), *il2rb-like* (ENSSSAG00000009526), and *id3* (ENSSSAG00000107585). The identity of T6 was more elusive. The array of markers detected implies a level of pluripotency, including several B cell lineage-determining transcription factors such as *ebf1* (ENSSSAG00000070298, ENSSSAG00000079780), *mef2c* (ENSSSAG00000032249, ENSSSAG00000066626), *bcl11aa/ab* (ENSSSAG00000078113/ENSSSAG00000086930, ENSSSAG00000119971), and *pax5* (ENSSSAG00000104911). The cluster was also marked by *cd37* (ENSSSAG00000065541) and *cd79a* (ENSSSAG00000113980). Furthermore, T6 was enriched for transcription factors regulating self-renewal, such as *msi2a* (ENSSSAG00000057624), *tcf7l2* (ENSSSAG00000066753), and *erg* (ENSSSAG00000006737) [85–87], as well as *cd9b* (ENSSSAG00000097341).

Finally, T10 (33 cells, 1 %) displayed the lowest expression of αβ T cell receptor genes, but high levels of the transcription factor *zbtb16* (alias *plzf* - ENSSSAG00000016597) and *gata2* (ENSSSAG00000079702), suggestive of an iNKT or innate lymphoid precursor subset [88,89].

In comparison to the expected separation of cd4 and cd8 positive T cells in the snRNA-seq data, *cd4-1*(ENSSSAG00000040774), *cd4-2* (ENSSSAG00000076595, ENSSSAG00000040842), and *cd8a* (ENSSSAG00000065860) enriched cells clustered together in scT1, most likely masking true heterogeneity within the cluster. Notably, individual cells did not co-express cd4 and cd8 transcripts. Similarly, *tcrg* (ENSSSAG00000100298) enriched cells clustered together in scT3. We find it

likely that further subclustering of these two clusters would have revealed subgroups similar to T2, T3, and T5 (scT1) or T4 and T9 (scT3), respectively. However, such subclustering was not performed due to the low number of cells recovered. In addition, scT6 shared a high number of marker genes with T11, including scavenger receptor M130 (ENSSSAG00000072601), *sox13* (ENSSSAG00000058488), and *il17rb* (ENSSSAG00000038993), supporting the existence of this presumed progenitor subset. Several of the remaining subsets (scT2, scT4, scT7, and scT8) showed varying enrichment of markers associated with the double-negative innate-like T cells in T6 and T7, among them ENSSSAG00000092386, *mef2cb* (ENSSSAG00000032249), *perforin-1-like* (ENSSSAG00000065678, ENSSSAG00000005439), and *il12rb* (ENSSSAG00000061284). It is not clear if these differences arise from the different size and development of fish, or can be partly attributed to methodological aspects, such as differences in nuclear and cytoplasmic transcript abundance.

3.5.3. *Head kidney endothelial cells show transcriptional profiles consistent with arterial, venous, scavenger and glomerular phenotypes*

Subclustering of the endothelial population revealed five distinct subclusters (Fig. 5A), all expressing high levels of endothelial-specific genes (Fig. 5B). List of markers in endothelial cell subclusters are shown in Supplementary Table 7. Again, all Ensembl IDs shown in the text were identified in the snRNA-seq dataset.

E1 (972 cells, 63 % of all endothelial cells) appears to represent scavenger capillary endothelium cells, with enrichment of several relevant marker genes including *stab2* (ENSSSAG00000045007), *c-type lectin domain family 4 member e-like* (ENSSSAG00000120844) and *mrc1* (ENSSSAG00000073565) [90]. An activated and phagocyte-like phenotype was further supported by enrichment of neurexins (*nrxn1* (ENSSSAG00000004275), *nrxn2* (ENSSSAG00000002870)) [91], *vcam1b* (ENSSSAG00000043624) [92], *csf1-2* (ENSSSAG00000078129) [93], and genes encoding lysosomal proteins (*cats* (ENSSSAG00000010327) and *lamp1* (ENSSSAG00000103986, ENSSSAG00000002337). The subcluster was also enriched for two genes typical of mammalian lymphatic endothelium, *lyve1b* (ENSSSAG00000005461) and *flt4* (ENSSSAG00000040805, ENSSSAG00000084309) [94,95].

Consistent with the notion that the majority of renal endothelial cells are of capillary origin, only three small clusters expressed high levels of the large vessel marker *vwf* (ENSSSAG00000101168) [94]. The large vessel-derived endothelial cells clustered in E3 (111 cells, 7 % of all endothelial cells), E4 (65 cells, 4 %), and E5 (25 cells, 2 %). The expression of *vwf* was strongest in E4, suggesting this subcluster represents the venous side of circulation [96]. This assumption was strengthened by enrichment for the venous markers *plvapb* (ENSSSAG00000040305) and *fscn1* (ENSSSAG00000093180) [94].

On the other hand, E3 likely represented the arterial side of circulation, based on enrichment of *gja5* (*gja5a* [ENSSSAG00000042461, ENSSSAG00000120725], *gja5b2* [ENSSSAG00000120725]), which in mouse is specific to arteries, driven by flow, and promotes arterial identity [94,97,98]. Furthermore, enrichment of *cldn5* (ENSSSAG00000120089) [94,98], *dll4* (ENSSSAG00000055522, ENSSSAG00000043356) [99], *efnb2a* (ENSSSAG00000049945) [100], *mecom* (ENSSSAG00000048049, ENSSSAG00000041461) [94], and *dlc* (ENSSSAG00000047939) [101] are consistent with an arterial phenotype.

The last endothelial subcluster was E2 (361 cells, 24 % of all endothelial cells), which could represent glomerular endothelium. Several E2-enriched genes have roles in cellular signaling (*nuggc* [ENSSSAG00000084919, ENSSSAG00000004114], *inpp4aa* [ENSSSAG00000080849], *prex1* [ENSSSAG00000108443, ENSSSAG00000044871], *vav3* [ENSSSAG00000077687, ENSSSAG00000045787, ENSSSAG00000067657], *fam65b* [ENSSSAG00000052730], *ptprc* [ENSSSAG00000066666], and *ptprsa* [ENSSSAG00000065535]). In addition, E2 was enriched for several B cell-typical genes, including *ebf1* (ENSSSAG00000070298, ENSSSAG00000079780), *cd79a* (ENSSSAG00000113980), *pax5* (ENSSSAG00000104911), and *cd37* (ENSSSAG00000065541). Interestingly, the transcription factor *ebf1* appears to be required for postnatal glomerular maturation [102]. Two additional glomerular marker genes were enriched in E2, *adgre5b.3* (ENSSSAG00000106051, ENSSSAG00000010801) and *syne1.b* (ENSSSAG00000070134) [94], strengthening the hypothesis that E2

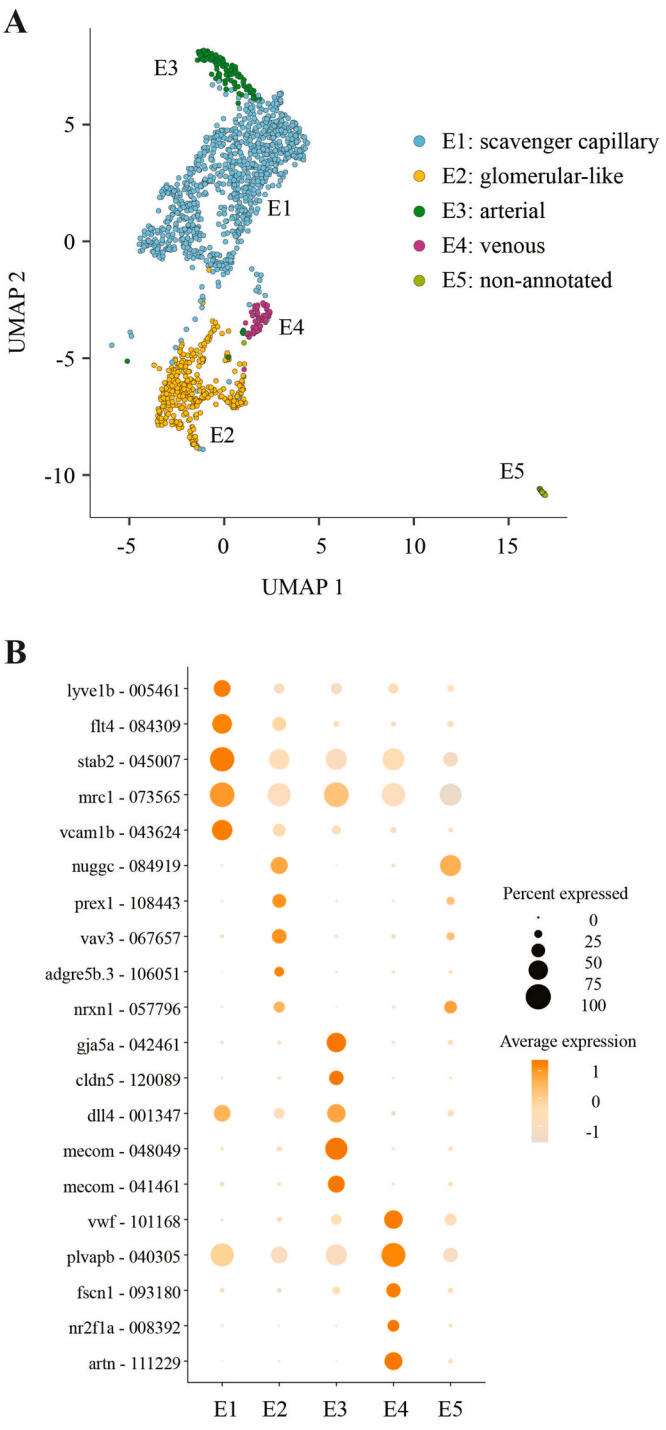

Fig. 5. *Subclustering of endothelial cells in the head kidney.* (A) UMAP of endothelial cell subclusters identified by snRNA-seq. (B) Dotplot displaying markers for each endothelial cell subcluster. The dot colours indicate the average normalised expression of the gene while the sizes of the dots corresponds to the percentage of cells expressing the gene in each subcluster. The number next to the gene name provides the last six digits of the Ensembl accession number.

cells are of glomerular origin, in agreement with their relative abundance [94].

3.5.4. Developmental trajectories from stems cells to distinct myeloid lineages

Clustering based on principal components failed to reveal biologically meaningful heterogeneity within the MP and granulocyte lineages. To test if these lineages had not yet undergone differentiation from immature states derived from the HSCs, we performed a trajectory analysis of the HSC, MP, and granulocyte populations using PHATE [26]. While the snRNA-seq dataset failed to display any clear trajectories (Supplementary Fig. 6), the scRNA-seq data identified two distinct branches from HSCs leading to granulocytes and MPs, with the granulocyte branch displaying a further bifurcation, which we named G2 and G3 (Fig. 6A). Clustering based on the PHATE embeddings revealed multiple intermediate populations between the HSCs for both the MP, i.e. MP (1) and MP (2), and granulocyte branches, i.e. G2 (1–4) and G3 (1–6) (Fig. 6A).

Marker genes for each sub-population defined by PHATE are provided in Supplementary Table 8. Marker genes for mature neutrophils including *mmp13* (ENSSSAG00000070495) and *ncf1* (ENSSSAG00000041940) showed increasing expression moving from HSCs towards both terminal granulocyte states, while marker genes for differentiated MPs including *cxcr3.2* (ENSSSAG00000063084) and *mpeg1* (ENSSSAG00000076214) exhibited increasing expression along the MP branch (Fig. 6B). Conversely, expression of the HSC markers *egr1* (ENSSSAG00000093647) and *nr4a1* (ENSSSAG00000045856) decreased along both lineages, and were completely silenced in both granulocyte branches (Fig. 6B). However, the terminal MP state MP (2) retained significant *nr4a1* expression, which is interesting considering that this transcription factor is involved in the differentiation of monocyte subpopulations in mammalian bone marrow [103]. We also found that two salmonid-specific paralogues encoding the Spi-1 (alias PU.1) transcription factor (ENSSSAG00000007573 and ENSSSAG00000064470), thought to drive the differentiation of mammalian stems cells into both neutrophils and monocytes [104], showed differential expression along the granulocyte and MP branches (Fig. 6B). Specifically, one paralogue (ENSSSAG00000007573) showed earlier and higher overall expression in both granulocyte branches. We observed that two paralogues encoding the transcription factor Mef2c (ENSSSAG00000032249 and ENSSSAG00000066626), shown previously to direct monocyte development and restrict granulocyte development [105], were upregulated in the intermediate monocyte state MP (1) (Fig. 6B). We further observed a change in expression of genes encoding enzymes representing granulocyte-stimulating factor targets in the earliest stage of the granulocyte branch (G1), including alkaline phosphatase (ENSSSAG00000081220) and myeloid-specific peroxidase (ENSSSAG00000048994) [106].

To understand the distinction between the two granulocyte trajectories, we performed differential expression tests between G2 (4) and G3 (6) (Supplementary Table 9). G3 showed a striking expression of interferon-stimulated genes, including *ifi27l2a* (ENSSSAG00000003797), *mx2* (ENSSSAG00000077530), four paralogues encoding polyubiquitin-like Isg15 (ENSSSAG00000064740, ENSSSAG00000105519, ENSSSAG00000098221, and ENSSSAG00000105254), and three paralogues encoding Rsad2 (ENSSSAG00000108937, ENSSSAG00000106505, and ENSSSAG00000108840) (Fig. 6C and D). According to findings from a study in zebrafish [107], neutrophils were the

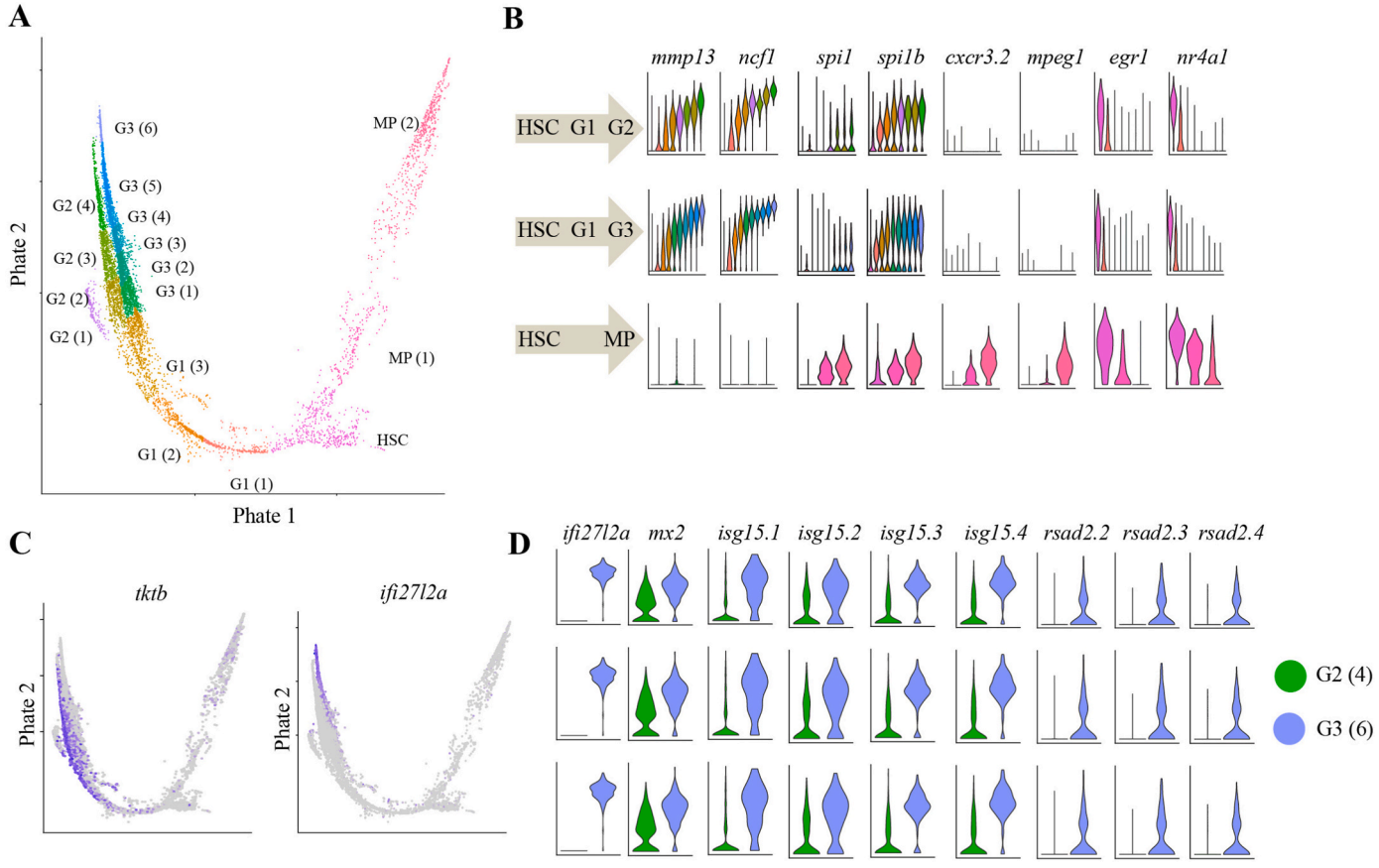

Fig. 6. *Trajectory analysis of HSC, MPs and Granulocytes.* (A) PHATE plot of the HSCs, MPs and granulocytes revealing a clear trajectory from HSCS to MPs, and a separate trajectory to the granulocytes, with an additional bifurcation into two populations, G2 and G3. (B) Violin plots of granulocyte and monocyte markers revealing increasing expression towards the terminal ends of the trajectory and reducing expression of HSC markers. (C) Visualisation of the differential expression of genes between G2 and G3, driving the annotation of independent populations. (D) Differential expression of selected interferon-stimulated genes between G2 and G3.

major cell population expressing type I interferon and involved in combating viral infections. These observations further strengthens the assumption that G3 represents neutrophils. G2 showed less obvious marker genes, with the most expressed gene encoding one of the gene duplicates encoding the metabolic enzyme transketolase (ENSSSAG00000095322), shown elsewhere to be important for neutrophil function [108].

4. Discussion

Over the last decade, an exponential rise in the availability and throughput of single cell transcriptomics has vastly increased our knowledge of the range and plasticity of cellular phenotypes and their roles in mammalian biology and pathology. Initiatives such as The Human Cell Atlas Project is currently building extensive atlases comprising multiple molecular measurements of all cell types in the human body [109]. The creation of widely available gene expression databases of signature genes of a multitude of cell types will enhance our understanding of the interplay between different cell types in a range of activation and differentiation states in health and disease.

Exploitation of single cell transcriptomics is also rapidly advancing biological knowledge in non-model fish species, improving our understanding of the immune system amongst many other traits [4,6]. Importantly, the identification of specific molecular targets also facilitates further characterisation of individual cell types in their natural morphological context, for example by *in situ* hybridisation. This is of particular value in species such as Atlantic salmon, where the availability of monoclonal antibodies is limited.

Using cutting-edge omics technique, we report a comprehensive atlas of Atlantic salmon head kidney cells using single cell transcriptomics. We provide a novel catalogue of robust marker genes for the annotation of all major cell types in the Atlantic salmon head kidney, which will be a useful reference for the research community, including fish immunologists. By comparing two datasets, one generated from cells (scRNA-seq) and one from nuclei (snRNA-seq), we identify markers that successfully annotate cell types using either approach, increasing the transferability of our findings to future studies. Moreover, we found that snRNA-seq detected a wider range of cell types than scRNA-seq, and that this loss was associated with sample preparation prior to library preparation. We here discuss our findings in the view of the current literature and highlight advantages and disadvantages of both techniques, with a particular view to their use in Atlantic salmon. For a more comprehensive discussion of the two techniques, we refer to a recent review [4].

It is already well established that scRNA-seq and snRNA-seq differ in both recovered cell types and specific gene enrichment, even when performed on the same sample, and it is becoming increasingly common to apply both techniques to achieve a more comprehensive understanding of the target tissue and cells. Directly comparing scRNA-seq and snRNA-seq data can be challenging due to disparities in cellular and nuclear expression patterns, as well as variations in cell type recovery. Thus, performing separate (rather than integrated) analyses for scRNA-seq and snRNA-seq data is thought to provide a more accurate understanding of cellular composition [110]. However, performing complementary analyses may be difficult to achieve in most aquaculture studies, due to the associated cost barriers. Our own attempts to integrate the scRNA-seq and snRNA-seq data resulted in anomalies when clustering, with significant mixing of unrelated lineages in the same clusters, indicating that independent analyses of the datasets was a better approach. In our study, eight major cell populations were identified in both our scRNA-seq and snRNA-seq datasets. In line with previous reports of differences in cell type recovery between the two methods [7,9,111,112], four additional cell populations were recovered by snRNA-seq only. Most considerations related to the description of specific cell types and markers are incorporated in the results section and will not be repeated here. However, the great discrepancy in cell type recovery between scRNA-seq and snRNA-seq datasets deserves attention and probably relates to insufficient tissue dissociation and trapping of cells during filtering of the single cell suspension prior to scRNA-seq library preparation. Before libraries can be prepared, tissues are dissociated by mechanical and/or enzymatic digestion, followed by filtering to ensure clean and viable single cell suspensions. This critical step can result in loss of rare and fragile cell types and may also trigger dissociation-induced stress responses [4]. Our protocol relied solely on mechanical dissociation to obtain single cell suspensions for library preparation. However, similar to scRNA-seq studies based on mechanical dissociation of the head kidney in three other fish species: three-spined stickleback [12], broadnosed pipefish [13], and flounder [16], our scRNA-seq analysis failed to recover endothelial cells. The strong reduction in endothelial marker transcripts observed during the filtering process indicates that mechanical dissociation of the head kidney may not be effective in dissociating structures like vascular stalks. It is plausible that the same could apply to the other cell types missing from the scRNA-seq analysis. Furthermore, potential effects of density gradient centrifugation on cell type recovery should be taken into consideration. Enzymatic digestion could address this limitation, based on previous analyses in zebrafish [113,114]. However, its inclusion could introduce new challenges: a study of mouse kidney showed that podocytes were absent or barely detectable when warm enzymatic dissociation was used [115]. The same study showed high expression of stress-induced genes, attributed to the dissociation process rather than the droplet-based library generation, as the same genes were induced in a parallel sample analysed by bulk RNA-seq. Such adverse responses could potentially be augmented in cold-adapted species such as Atlantic salmon, and a careful optimization of cold-active enzymes would be required before implementing enzymatic tissue disruption [4]. Finally, new techniques like FixNCut, which applies fixation of the tissue prior to cell dissociation, could help limit artifacts introduced during handling and improve the range of cell types detected by scRNA-seq [116].

While studies in mammals have suggested a bias towards preferential detection of immune cells when using scRNA-seq [111,112,117], our snRNA-seq dataset recovered six times more T cells than scRNA-seq and more than twice the number of MPs. It is tempting to speculate that the dissociation method chosen for our study could have influenced the relative numbers of immune cells in scRNA-seq. Indeed, the relative proportion of several recovered cell types was different in our two datasets. While B cells, NK-like cells, and HSCs were recovered in similar proportions, granulocytes were more abundant in the scRNA-seq dataset, while the remaining eight cell types were more abundant in the snRNA-seq dataset. Nevertheless, an important limitation of our study is the difference in samples used to compare scRNA-seq and snRNA-seq, representing fish of different body sizes sampled from distinct populations. This makes it impossible to exclude that some of the reported differences between datasets result from ontogenetic differences [118]. Thus, to draw standardized conclusions about biases between scRNA-seq and snRNA-seq, parallel sequencing of samples from the same animals will be necessary. Nevertheless, our data shows that snRNA-seq is well suited to detect most cell types in the Atlantic salmon head kidney.

One advantage of single-cell omics, especially when working with non-model animals, is the ability to cluster and annotate cell types without extensive prior knowledge of marker genes. Our extended lists of marker genes for the 12 major cell populations of the Atlantic salmon head kidney represent an important resource that will help identify key markers for use in other studies and aid the choice of cell-specific targets for development of antibodies and probes for *in situ* hybridisation. Here, we have identified robust and novel markers for specific cell populations. For instance, the gene *mcr1* (ENSSSAG00000073565) was found to be exclusively expressed in endothelial cells, whereas its paralog, *mcr1b* (ENSSSAG00000039787), showed expression in MPs instead of endothelial cells. This provides new insights into the differential expression patterns of paralogues in different cell populations in Atlantic salmon head kidney.

Furthermore, our observations enable us to reevaluate markers used

in Atlantic salmon studies. Our results indicate that some cell type markers may be less specific than commonly assumed, at least on the transcript level. For example, the pan-B cell markers *cd79a* and *cd22* were both expressed in B cells, but neither was restricted to B cells only. While *cd79a* was a marker in one T cell subcluster (T6), paralogues of the *cd22* gene were expressed by erythrocytes and granulocytes. This is supported by previous single reports: a study by Hashimoto et al. [119] demonstrated that CD79a is transiently expressed in immature T lineage cells, and *cd22* expression has been reported in erythrocytes and lymphocytes of maraena whitefish (*Coregonus maraena*) and mice granulocytes [120,121]. This highlights the importance of accurately defining which paralogues are expressed in each cell population. Such information is crucial for downstream applications like *in situ* hybridisation, where selecting and specifically capturing the most appropriate target gene is essential for the success and accuracy of the experiment.

Compared to mammals, limited information is available about the different subsets of immune cells in Atlantic salmon and their development. Our subclustering of B and T cell clusters revealed distinct groups of head kidney lymphocytes, linked to biologically relevant subtypes. The heterogeneity of rainbow trout peripheral blood B cells was recently examined by scRNA-seq [122], describing B cell differentiation stages subsequent to leaving the head kidney. However, to our knowledge, no studies published to date have used single cell transcriptomics to dissect immune cell heterogeneity within the salmonid head kidney, which is the main organ for B cell lymphopoiesis. Our findings increase the understanding of salmonid B cell biology by complementing previous characterisations of rainbow trout B cells. These studies used cytometric to assess key transcription factors, surface immunoglobulins, and cell size, separating rainbow trout head kidney B cells into "early development B cells" (*rag1*$^{+}$*ebf1*$^{+}$, equivalent to our B1 population), "late development B cells" (*pax5*$^{+}$*hcmu*$^{+}$, equivalent to our B3 and B4 populations), and "plasmablasts/pre-plasma cells and plasma cells" (equivalent to our B5) [44,45]. In addition, our findings suggest that B2 represents proliferating pre-B cells, the developmental stage following B1. B3 and B4 showed enrichment for the quiescence-associated transcription factor *klf2*, typical of naïve, follicular B cells and B1 B cell lineage in mammals [123,124], as well as *dnmt3a/b*, encoding DNA methylases that limit plasma cell differentiation [57]. However, the populations differed in their immunoglobulin profiles. Only B4 expressed the gene encoding the heavy chain of mucosal immunoglobulin IgT, suggesting that B3 and B4 represent alternative rather than sequential differentiation paths. It may be worth noting that transcription profiles of naïve and memory B cells have many features in common, and it is possible that further subclustering of B3 and/or B4 populations would have revealed memory B cell, as well as pre-immune subsets [125]. Supporting the validity of our interpretations, similar B cell populations to B3, B4 and B5 (but not B1 and B2) were identified by snRNA-seq in the spleen from the same fish in a separate study [18], in line with their proposed nature.

Our data also provide a snapshot of the transcription factors enriched at each developmental stage of salmonid B cell lymphopoiesis. This detailed analysis allows capture of high-resolution information regarding the expression patterns of a range of transcription factors, inviting further dissection of the regulatory transcriptional networks involved. The transcription factor program that guides B cell lymphopoiesis appears to be highly conserved amongst vertebrates, as well as tightly controlled, amongst other by the use of alternative splice variants [44]. The read length and depth provided by our protocol is not optimal to evaluate the use of alternative splicing, however, we observed that different gene duplicates of several transcription factors with established roles in B cell development were enriched at different stages of differentiation. For example, different orthologues of *ebf1*, a key regulator of the B cell transcriptional program [126], showed reciprocal expression patterns between B1 and later developmental stages. While ENSSSAG00000070298 was enriched in B1 and thereafter declined, ENSSSAG00000079780 was not upregulated until after pre-BCR proliferation with the strongest expression seen in B3. A third *ebf1* duplicate, ENSSSAG00000041858, followed the same pattern as ENSSSAG00000079780, but was expressed in a smaller proportion of cells. Interestingly, two gene duplicates of *bcl11a*, a driver of *ebf1* expression [61] followed the same pattern, as *bcl11aa* was enriched in B1, and the alternative gene duplicate *bcl11ab* increased later, with enrichment in B3. Further studies are needed to understand if there is a causal relationship between these observations, and if this apparent switch in transcription factor expression has biological significance. Our dataset represents a resource for researchers interested in studying the regulation of salmonid B cell development, as well as a springboard for further focused studies.

Despite extensive characterisation of T cell receptor diversity at the genomic level [74,127] and an array of antibody-based analyses of T cell surface antigens (summarised in Ref. [128]), our understanding of salmonid head kidney T cell heterogeneity is still limited by the availability of specific reagents and knowledge of subtype-specific targets. Recent scRNA-seq studies in two other teleosts, Nile tilapia [14] and flounder [16], have identified *cd4*$^{-}$*cd8*$^{-}$, *cd4*$^{-}$*cd8*$^{+}$, *cd4*$^{+}$*cd8*$^{-}$, and *cd4*$^{+}$*cd8*$^{+}$ (Nile tilapia only) T cell subsets in head kidney, as well as cells with low expression of *cd4/cd8*, proposed to represent immature T cells. Our findings are in line with these studies, showing *cd4*+*cd8*- (T2 and T5), *cd4-cd8*+ (T3), and a low *cd4/cd8* expressing T cell subset that could represent immature T cells (T1). We also extend on these observations by identifying a separate subset of *cd4*+ Tregs that express *foxp3*, and attempting to classify the double negative populations (T4-T11) further. In this group of clusters, two exhibited profiles suggestive of distinct γδT cell populations, while at least one resembled mammalian innate-like cytotoxic T cells [84] (T7), and two resembled lymphoid progenitor populations (T10 and T11). The expression of B cell lineage markers in the final subcluster (T6) is difficult to explain, but could be related to a state of self-renewal, as some reports suggest an association with or involvement in the regulation of proliferation and survival in immature or transformed T cells [119,129–131]. Our data can be used to develop new approaches to understand T cell subsets in salmonids. For example, the combined detection of *tcrγ*, *il17rb*, and *m130* could be tested as a strategy to enrich and separate low frequency *cd3e* + T cell subsets of the γδT lineage (T11: *tcrγ*$^{-}$*il17rb* + *m130*$^{+}$; T4: *tcrγ*$^{+}$*il17rb*$^{-}$*m130*$^{+}$;T9: *tcrγ*$^{+}$*il17rb*$^{-}$*m130*$^{-}$). As these three candidate genes all encode putative surface proteins, they could also be candidates for antibody-based separation prior to functional testing, bearing in mind that regulation of translation, protein half-life, and surface expression may disturb the clean distinction observed on the transcript level. Interestingly, T cell populations with similar profiles to all clusters identified in our study except T6 and T10 were identified by snRNA-seq of the spleen of the same fish in a separate study [18].

We also performed subclustering of the endothelial cells, illustrating diversity in a non-immune cell population with important roles in fish physiology. Endothelial cells are the target of several infectious agents, such as isavirus salaris (infectious salmon anaemia virus) and viral haemorrhagic septicaemia virus [132,133]. Our study confirms that a significant proportion of head kidney endothelial cells have a transcription profile suggestive of a scavenging phenotype, in line with past experimental work [134] and reveals target genes that will aid the identification of these cells in subsequent studies.

Similar to previous reports, our scRNA-seq and snRNA-seq datasets showed variation in the number of differentially expressed genes recovered. Furthermore, the two intracellular compartments differed in their content of specific transcripts. While nuclear RNA tends to be enriched for long intergenic noncoding RNAs and nuclear-function genes, scRNA-seq captures more ribosomal and mitochondrial genes [111,135]. The capture of high amounts of ribosomal and mitochondrial genes in scRNA-seq analysis is expected, as the whole cell is used for library preparation. Cells with a high ribosomal and mitochondrial content are commonly considered technical artifacts indicative of low-quality samples, and hence discarded during filtering. However, our

findings suggest caution must be applied when choosing such a threshold to avoid excluding genuine cells. Our scRNA-seq dataset showed that HSCs and some immune cells (MPs, B cells, and T cells) had the highest content of ribosomal transcripts. This is in accordance with previous studies that have demonstrated how immune cells tend to express higher levels of ribosomal genes to support cell proliferation and activation [136]. Furthermore, early stage HSCs exhibited elevated transcription of ribosomal genes, which becomes suppressed during differentiation when lineage-specific genes are upregulated [137]. The lower detection of ribosomal and mitochondrial transcripts is a clear advantage of snRNA-seq, leaving more sequencing coverage to detect cell identity-relevant transcripts and possibly enhancing cell-type identification.

Ambient RNA is a term used to describe RNA molecules in the suspension that have been released from dead or stressed cells, and when incorporated in droplets produced by single cell microfluidic platforms can be wrongly counted as cells. The levels of ambient RNA were highest in our snRNA-seq dataset. Similar to others before us, we concluded that snRNA-seq requires more rigorous background removal methods to distinguish between droplets filled with ambient RNA and those containing actual cells. However, we found that the overall annotation of major cell types detected by scRNA-seq and snRNA-seq in our data was consistent. This shows that snRNA-seq provides sufficient gene detection to enable the identification of distinct cell populations in Atlantic salmon head kidney, despite capturing a lower total RNA content, but does not indicate that it is superior to scRNA-seq in this respect.

In conclusion, this study is the first to analyze head kidney of Atlantic salmon by single-cell transcriptomics. To our knowledge, it is the first study to compare cell type detection and gene expression obtained by two sample isolation and library preparation techniques, scRNA-seq and snRNA-seq, in a salmonid species. Our findings represent an important contribution to aquaculture research and fish immunology, by expanding understanding of the cellular composition of Atlantic salmon head kidney and cell type-specific expression profiles, and by delivering a comprehensive catalogue of marker genes that can be used as targets for antibody generation and probes for *in situ* RNA hybridisation. Furthermore, the insights gained from this study will aid researchers in making informed decisions about which single cell transcriptome method is most suitable to effectively address their research questions.

Funding

The study was funded by grants from the Research Council Norway (ID:302191), the University of Edinburgh's Data Driven Innovation Initiative (Scottish Funding Council Beacon 'Building Back Better' Call), and the Biotechnology and Biological Sciences Research Council, including the institutional strategic programme grants BBS/E/D/10002071, BBS/E/RL/230001C, BBS/E/D/20002174, BBS/E/RL/230002B, and the responsive mode grants BB/W005859/1 and BB/W008564/1. NH is supported by a Wellcome Trust Senior Research Fellowship in Clinical Science (ref. 219542/Z/19/Z). UG is supported by the Research Council of Norway (ID:274635).

Ethics

Norway - All the procedures were conducted in agreement with the regulations enforced by the National Animal Research Authority, and protocols were approved by the Norwegian Food Safety Authority FOTS (ID: 24382).

Scotland - Animal work was carried out in compliance with the Animals (Scientific Procedures) Act 1986 under Home Office licence PFF8CC5BE and was approved by the ethics committee of the University of Aberdeen.

CRediT authorship contribution statement

Adriana M.S. Andresen: Conceptualization, Methodology, Validation, Investigation, Formal analysis, Writing – original draft, Visualization, Data curation. **Richard S. Taylor:** Conceptualization, Methodology, Validation, Investigation, Formal analysis, Writing – original draft, Visualization, Data curation. **Unni Grimholt:** Writing – review & editing. **Rose Ruiz Daniels:** Investigation, Writing – review & editing. **Jianxuan Sun:** Investigation, Writing – review & editing. **Ross Dobie:** Investigation. **Neil C. Henderson:** Resources, Project administration, Supervision. **Samuel A.M. Martin:** Resources, Writing – review & editing. **Daniel J. Macqueen:** Conceptualization, Methodology, Project administration, Visualization, Resources, Funding acquisition, Supervision, Writing – original draft. **Johanna H. Fosse:** Conceptualization, Methodology, Project administration, Visualization, Resources, Funding acquisition, Supervision, Writing – original draft.

Data availability

The data discussed in this publication have been deposited in NCBI's Gene Expression Omnibus and are accessible through GEO Series accession number GSE253087. Codes used for running experiments and plotting are publicly available on GitHub repository at github.com/NorwegianVeterinaryInstitute/Salmon_HK_SingleCellSeq.

Acknowledgements

We would like to thank Inger Austrheim Heffernan and the bioinformaticians at the Norwegian Veterinary Institute for technical assistance, and Ricardo Tavares Benicio and Bjørn-Reidar Hansen (the aquaculture research station, NMBU, Ås, Norway) for providing fish. We are also grateful for the sequencing/microarray services provided by the Helse Sør-Øst Genomics Core Facility at Oslo University Hospital. Computations resources used for preliminary analysis were provided by Sigma2 - the National Infrastructure for High Performance Computing and Data Storage in Norway. Finally, we would like to thank Carolina Tafalla (Animal Health Research Centre, Valdeolmos, Spain) for fruitful discussions regarding interpretation of B cell data.

Appendix A. Supplementary data

Supplementary data to this article can be found online at https://doi.org/10.1016/j.fsi.2024.109357.

References

[1] B. Dixon, Vaccines for finfish aquaculture: what do we need to know to make them work? Electron. J. Biotechnol. 15 (2012), 14-14.
[2] X. Qian, Y. Ba, Q. Zhuang, G. Zhong, RNA-Seq technology and its application in fish transcriptomics, OMICS 18 (2) (2014) 98–110.
[3] F. Tang, C. Barbacioru, Y. Wang, E. Nordman, C. Lee, N. Xu, X. Wang, J. Bodeau, B. Tuch, A. Siddiqui, K. Lao, M. Surani, mRNA-Seq whole-transcriptome analysis of a single cell, Nat. Methods 6 (2009) 377–382.
[4] R.R. Daniels, R.S. Taylor, D. Robledo, D.J. Macqueen, Single cell genomics as a transformative approach for aquaculture research and innovation, Rev. Aquacult. (2023).
[5] E. Papalexi, R. Satija, Single-cell RNA sequencing to explore immune cell heterogeneity, Nat. Rev. Immunol. 18 (1) (2018) 35–45.
[6] J.T.H. Chan, S. Kadri, B. Köllner, A. Rebl, T. Korytář, RNA-seq of single fish cells – seeking out the leukocytes mediating immunity in teleost fishes, Front. Immunol. 13 (2022 Jan 24) 798712, https://doi.org/10.3389/fimmu.2022.798712. eCollection.2022.
[7] T.E. Bakken, R.D. Hodge, J.A. Miller, Z. Yao, T.N. Nguyen, B. Aevermann, E. Barkan, D. Bertagnolli, T. Casper, N. Dee, E. Garren, J. Goldy, L.T. Graybuck, M. Kroll, R.S. Lasken, K. Lathia, S. Parry, C. Rimorin, R.H. Scheuermann, N. J. Schork, S.I. Shehata, M. Tieu, J.W. Phillips, A. Bernard, K.A. Smith, H. Zeng, E. S. Lein, B. Tasic, Single-nucleus and single-cell transcriptomes compared in matched cortical cell types, PLoS One 13 (12) (2018) e0209648.
[8] N. Thrupp, C. Sala Frigerio, L. Wolfs, N.G. Skene, N. Fattorelli, S. Poovathingal, Y. Fourne, P.M. Matthews, T. Theys, R. Mancuso, B. de Strooper, M. Fiers, Single-nucleus RNA-seq is not suitable for detection of microglial activation genes in humans, Cell Rep. 32 (13) (2020) 108189.

[9] H. Wu, Y. Kirita, E.L. Donnelly, B.D. Humphreys, Advantages of single-nucleus over single-cell RNA sequencing of adult kidney: rare cell types and novel cell states revealed in fibrosis, J. Am. Soc. Nephrol. 30 (1) (2019) 23–32.

[10] H. Bjørgen, E.O. Koppang, Anatomy of teleost fish immune structures and organs, Immunogenetics 73 (1) (2021) 53–63.

[11] C.M. Press, Ø. Evensen, The morphology of the immune system in teleost fishes, Fish Shellfish Immunol. 9 (4) (1999) 309–318.

[12] L.E. Fuess, D.I. Bolnick, Single-cell RNA sequencing reveals microevolution of the stickleback immune system, Genome Biology and Evolution 15 (4) (2023).

[13] J. Parker, N.C. Guslund, S. Jentoft, O. Roth, Characterization of pipefish immune cell populations through single-cell transcriptomics, Front. Immunol. 13 (2022), 820152-820152.

[14] L. Wu, A. Gao, L. Li, J. Chen, J. Li, J. Ye, A single-cell transcriptome profiling of anterior kidney leukocytes from nile Tilapia (Oreochromis niloticus), Front. Immunol. 12 (2021).

[15] J. Niu, Y. Huang, X. Liu, Z. Zhang, J. Tang, B. Wang, Y. Lu, J. Cai, J. Jian, Single-cell RNA-seq reveals different subsets of non-specific cytotoxic cells in teleost, Genomics 112 (6) (2020) 5170–5179.

[16] H. Tian, J. Xing, X. Tang, X. Sheng, H. Chi, W. Zhan, Single-cell transcriptome uncovers heterogeneity and immune responses of leukocytes after vaccination with inactivated Edwardsiella tarda in flounder (Paralichthys olivaceus), Aquaculture 566 (2023) 739238.

[17] R.S. Taylor, R. Ruiz Daniels, R. Dobie, S. Naseer, T.C. Clark, N.C. Henderson, P. Boudinot, S.A.M. Martin, D.J. Macqueen, Single cell transcriptomics of Atlantic salmon (Salmo salar L.) liver reveals cellular heterogeneity and immunological responses to challenge by Aeromonas salmonicida, Front. Immunol. 13 (2022).

[18] J. Sun, R. Ruiz Daniels, A. Balic, A.M.S. Andresen, H. Bjørgen, R. Dobie, N. C. Henderson, E.O. Koppang, S.A.M. Martin, J.H. Fosse, R.S. Taylor, D. J. Macqueen, Cell atlas of the Atlantic salmon spleen reveals immune cell heterogeneity and cell-specific responses to bacterial infection, Fish Shellfish Immunol. (2024) 109358.

[19] R. Ruiz Daniels, R.S. Taylor, R. Dobie, S. Salisbury, J.J. Furniss, E. Clark, D. J. Macqueen, D. Robledo, A versatile nuclei extraction protocol for single nucleus sequencing in non-model species–Optimization in various Atlantic salmon tissues, PLoS One 18 (9) (2023) e0285020.

[20] B. Kaminow, D. Yunusov, A. Dobin, STARsolo: accurate, fast and versatile mapping/quantification of single-cell and single-nucleus RNA-seq data, bioRxiv (2021), 2021.05.05.442755.

[21] S. Fleming, J. Marioni, M. Babadi, CellBender Remove-Background: A Deep Generative Model for Unsupervised Removal of Background Noise from scRNA-Seq Datasets, 2019.

[22] R. Satija, J.A. Farrell, D. Gennert, A.F. Schier, A. Regev, Spatial reconstruction of single-cell gene expression data, Nat. Biotechnol. 33 (5) (2015) 495–502.

[23] P. Germain, A. Lun, W. Macnair, M. Robinson, Doublet identification in single-cell sequencing data using scDblFinder [version 1; peer review: 1 approved, 1 approved with reservations], F1000Research 10 (979) (2021).

[24] I. Korsunsky, N. Millard, J. Fan, K. Slowikowski, F. Zhang, K. Wei, Y. Baglaenko, M. Brenner, P.-r. Loh, S. Raychaudhuri, Fast, sensitive and accurate integration of single-cell data with Harmony, Nat. Methods 16 (12) (2019) 1289–1296.

[25] R.J. Kinsella, A. Kähäri, S. Haider, J. Zamora, G. Proctor, G. Spudich, J. Almeida-King, D. Staines, P. Derwent, A. Kerhornou, P. Kersey, P. Flicek, Ensembl BioMarts: a Hub for Data Retrieval across Taxonomic Space, Database (Oxford), 2011 bar030.

[26] K.R. Moon, D. van Dijk, Z. Wang, S. Gigante, D.B. Burkhardt, W.S. Chen, K. Yim, A.v.d. Elzen, M.J. Hirn, R.R. Coifman, N.B. Ivanova, G. Wolf, S. Krishnaswamy, Visualizing structure and transitions in high-dimensional biological data, Nat. Biotechnol. 37 (12) (2019) 1482–1492.

[27] S. Lien, B.F. Koop, S.R. Sandve, J.R. Miller, M.P. Kent, T. Nome, T.R. Hvidsten, J. S. Leong, D.R. Minkley, A. Zimin, F. Grammes, H. Grove, A. Gjuvsland, B. Walenz, R.A. Hermansen, K. von Schalburg, E.B. Rondeau, A. Di Genova, J.K.A. Samy, J. Olav Vik, M.D. Vigeland, L. Caler, U. Grimholt, S. Jentoft, D. Inge Våge, P. de Jong, T. Moen, M. Baranski, Y. Palti, D.R. Smith, J.A. Yorke, A.J. Nederbragt, A. Tooming-Klunderud, K.S. Jakobsen, X. Jiang, D. Fan, Y. Hu, D.A. Liberles, R. Vidal, P. Iturra, S.J.M. Jones, I. Jonassen, A. Maass, S.W. Omholt, W. S. Davidson, The Atlantic salmon genome provides insights into rediploidization, Nature 533 (7602) (2016) 200–205.

[28] D.J. Macqueen, I.A. Johnston, A well-constrained estimate for the timing of the salmonid whole genome duplication reveals major decoupling from species diversification, Proc. Biol. Sci. 281 (1778) (2014) 20132881.

[29] R.S. Taylor, R.R. Daniels, D.P. Morata, M.K. Gundappa, D.J. Macqueen, Evolution of ray-finned fish genomes: status and directions with a primer on microRNA characterization, in: I.F. Monzón, J.M.O. Fernandes (Eds.), Cellular and Molecular Approaches in Fish Biology, Academic Press, 2022, pp. 309–346.

[30] L.-H. Johansen, M.K. Dahle, Ø. Wessel, G. Timmerhaus, M. Løvoll, M. Røsæg, S. M. Jørgensen, E. Rimstad, A. Krasnov, Differences in gene expression in Atlantic salmon parr and smolt after challenge with Piscine orthoreovirus (PRV), Mol. Immunol. 73 (2016) 138–150.

[31] L.H. Johansen, M.K. Dahle, O. Wessel, G. Timmerhaus, M. Lovoll, M. Rosaeg, S. M. Jorgensen, E. Rimstad, A. Krasnov, Differences in gene expression in Atlantic salmon parr and smolt after challenge with Piscine orthoreovirus (PRV), Mol. Immunol. 73 (2016) 138–150.

[32] A.C. West, Y. Mizoro, S.H. Wood, L.M. Ince, M. Iversen, E.H. Jørgensen, T. Nome, S.R. Sandve, S.A.M. Martin, A.S.I. Loudon, D.G. Hazlerigg, Immunologic profiling of the atlantic salmon gill by single nuclei transcriptomics, Front. Immunol. 12 (1480) (2021).

[33] Q. Di, Q. Lin, Z. Huang, Y. Chi, X. Chen, W. Zhang, Y. Zhang, Zebrafish nephrosin helps host defence against *Escherichia coli* infection, Open Biology 7 (8) (2017) 170040.

[34] N. Kim, A. Saudemont, L. Webb, M. Camps, T. Ruckle, E. Hirsch, M. Turner, F. Colucci, The p110delta catalytic isoform of PI3K is a key player in NK-cell development and cytokine secretion, Blood 110 (9) (2007) 3202–3208.

[35] J.V. Goldstone, M. Sundaramoorthy, B. Zhao, M.R. Waterman, J.J. Stegeman, D. C. Lamb, Genetic and structural analyses of cytochrome P450 hydroxylases in sex hormone biosynthesis: sequential origin and subsequent coevolution, Mol. Phylogenet. Evol. 94 (Pt B) (2016) 676–687.

[36] L.-Y. Zhou, D.-S. Wang, T. Kobayashi, A. Yano, B. Paul-Prasanth, A. Suzuki, F. Sakai, Y. Nagahama, A novel type of P450c17 lacking the lyase activity is responsible for C21-steroid biosynthesis in the fish ovary and head kidney, Endocrinology 148 (9) (2007) 4282–4291.

[37] A. Griffin, S. Parajes, M. Weger, A. Zaucker, A.E. Taylor, D.M. O'Neil, F. Müller, N. Krone, Ferredoxin 1b (Fdx1b) is the essential mitochondrial redox partner for cortisol biosynthesis in zebrafish, Endocrinology 157 (3) (2016) 1122–1134.

[38] C. Chai, Y.-w. Liu, W.-K. Chan, Ff1b is required for the development of steroidogenic component of the zebrafish interrenal organ, Dev. Biol. 260 (1) (2003) 226–244.

[39] C. Gistelinck, R. Gioia, A. Gagliardi, F. Tonelli, L. Marchese, L. Bianchi, C. Landi, L. Bini, A. Huysseune, P.E. Witten, A. Staes, K. Gevaert, N. De Rocker, B. Menten, F. Malfait, S. Leikin, S. Carra, R. Tenni, A. Rossi, A. De Paepe, P. Coucke, A. Willaert, A. Forlino, Zebrafish collagen type I: molecular and biochemical characterization of the major structural protein in bone and skin, Sci. Rep. 6 (2016) 21540.

[40] B. Li, Y.-W. Zheng, Y. Sano, H. Taniguchi, Evidence for Mesenchymal–Epithelial transition associated with mouse hepatic stem cell differentiation, PLoS One 6 (2) (2011) e17092.

[41] G.F. Gerlach, R.A. Wingert, Kidney organogenesis in the zebrafish: insights into vertebrate nephrogenesis and regeneration, Wiley Interdiscip Rev Dev Biol 2 (5) (2013) 559–585.

[42] S.C. Chan, Y. Zhang, M. Pontoglio, P. Igarashi, Hepatocyte nuclear factor-1β regulates Wnt signaling through genome-wide competition with β-catenin/lymphoid enhancer binding factor, Proc. Natl. Acad. Sci. USA 116 (48) (2019) 24133–24142.

[43] V. Sander, L. Salleh, R.W. Naylor, W. Schierding, D. Sontam, J.M. O'Sullivan, A. J. Davidson, Transcriptional profiling of the zebrafish proximal tubule, Am. J. Physiol. Ren. Physiol. 317 (2) (2019) F478–F488.

[44] P. Zwollo, Dissecting teleost B cell differentiation using transcription factors, Dev. Comp. Immunol. 35 (9) (2011) 898–905.

[45] P. Zwollo, K. Mott, M. Barr, Comparative analyses of B cell populations in trout kidney and mouse bone marrow: establishing "B cell signatures", Dev. Comp. Immunol. 34 (12) (2010) 1291–1299.

[46] D. Morgan, V. Tergaonkar, Unraveling B cell trajectories at single cell resolution, Trends Immunol. 43 (3) (2022) 210–229.

[47] R.H. Amin, M.S. Schlissel, Foxo1 directly regulates the transcription of recombination-activating genes during B cell development, Nat. Immunol. 9 (6) (2008) 613–622.

[48] R. Yücel, C. Kosan, F. Heyd, T. Möröy, Gfi1:Green fluorescent protein knock-in mutant reveals differential expression and autoregulation of the growth factor independence 1 (Gfi1) gene during lymphocyte development, J. Biol. Chem. 279 (39) (2004) 40906–40917.

[49] R.D. Lee, S.A. Munro, T.P. Knutson, R.S. LaRue, L.M. Heltemes-Harris, M. A. Farrar, Single-cell analysis of developing B cells reveals dynamic gene expression networks that govern B cell development and transformation, bioRxiv (2020), 2020.06.30.178301.

[50] F. Zou, X. Wang, X. Han, G. Rothschild, S.G. Zheng, U. Basu, J. Sun, Expression and function of tetraspanins and their interacting partners in B cells, Front. Immunol. 9 (2018) 1606.

[51] K. Tokoyoda, T. Egawa, T. Sugiyama, B.-I. Choi, T. Nagasawa, Cellular niches controlling B lymphocyte behavior within bone marrow during development, Immunity 20 (6) (2004) 707–718.

[52] T.A. Schwickert, H. Tagoh, S. Gültekin, A. Dakic, E. Axelsson, M. Minnich, A. Ebert, B. Werner, M. Roth, L. Cimmino, R.A. Dickins, J. Zuber, M. Jaritz, M. Busslinger, Stage-specific control of early B cell development by the transcription factor Ikaros, Nat. Immunol. 15 (3) (2014) 283–293.

[53] S. Herzog, M. Reth, H. Jumaa, Regulation of B-cell proliferation and differentiation by pre-B-cell receptor signalling, Nat. Rev. Immunol. 9 (3) (2009) 195–205.

[54] D.M. Page, V. Wittamer, J.Y. Bertrand, K.L. Lewis, D.N. Pratt, N. Delgado, S. E. Schale, C. McGue, B.H. Jacobsen, A. Doty, Y. Pao, H. Yang, N.C. Chi, B. G. Magor, D. Traver, An evolutionarily conserved program of B-cell development and activation in zebrafish, Blood 122 (8) (2013) e1–e11.

[55] S.M. Aukema, R. Siebert, E. Schuuring, G.W. van Imhoff, H.C. Kluin-Nelemans, E.-J. Boerma, P.M. Kluin, Double-hit B-cell lymphomas, Blood 117 (8) (2011) 2319–2331.

[56] M.C. Ordás, R. Castro, B. Dixon, J.O. Sunyer, S. Bjork, J. Bartholomew, T. Korytar, B. Köllner, A. Cuesta, C. Tafalla, Identification of a novel CCR7 gene in rainbow trout with differential expression in the context of mucosal or systemic infection, Dev. Comp. Immunol. 38 (2) (2012) 302–311.

[57] B.G. Barwick, C.D. Scharer, R.J. Martinez, M.J. Price, A.N. Wein, R.R. Haines, A. P.R. Bally, J.E. Kohlmeier, J.M. Boss, B cell activation and plasma cell differentiation are inhibited by de novo DNA methylation, Nat. Commun. 9 (1) (2018) 1900.

[58] C. Tafalla, L. González, R. Castro, A.G. Granja, B cell-activating factor regulates different aspects of B cell functionality and is produced by a subset of splenic B cells in teleost fish, Front. Immunol. 8 (2017).

[59] J.D. Hansen, E.D. Landis, R.B. Phillips, Discovery of a unique Ig heavy-chain isotype (IgT) in rainbow trout: implications for a distinctive B cell developmental pathway in teleost fish, Proc. Natl. Acad. Sci. USA 102 (19) (2005) 6919–6924.

[60] I. Györy, S. Boller, R. Nechanitzky, E. Mandel, S. Pott, E. Liu, R. Grosschedl, Transcription factor Ebf1 regulates differentiation stage-specific signaling, proliferation, and survival of B cells, Genes Dev. 26 (7) (2012) 668–682.

[61] P. Liu, J.R. Keller, M. Ortiz, L. Tessarollo, R.A. Rachel, T. Nakamura, N. A. Jenkins, N.G. Copeland, Bcl11a is essential for normal lymphoid development, Nat. Immunol. 4 (6) (2003) 525–532.

[62] J. Ye, I. Kaattari, S. Kaattari, Plasmablasts and plasma cells: reconsidering teleost immune system organization, Dev. Comp. Immunol. 35 (12) (2011) 1273–1281.

[63] A.L. Shaffer, K.-I. Lin, T.C. Kuo, X. Yu, E.M. Hurt, A. Rosenwald, J.M. Giltnane, L. Yang, H. Zhao, K. Calame, L.M. Staudt, Blimp-1 orchestrates plasma cell differentiation by extinguishing the mature B cell gene expression program, Immunity 17 (1) (2002) 51–62.

[64] F. Di Rosa, T. Gebhardt, Bone marrow T cells and the integrated functions of recirculating and tissue-resident memory T cells, Front. Immunol. 7 (2016) 51.

[65] F. Takizawa, S. Magadan, D. Parra, Z. Xu, T. Korytář, P. Boudinot, J.O. Sunyer, Novel teleost CD4-bearing cell populations provide insights into the evolutionary origins and primordial roles of CD4+ lymphocytes and CD4+ macrophages, J. Immunol. 196 (11) (2016) 4522–4535.

[66] Jonathan H. Esensten, Ynes A. Helou, G. Chopra, A. Weiss, Jeffrey A. Bluestone, CD28 costimulation: from mechanism to therapy, Immunity 44 (5) (2016) 973–988.

[67] M.K. Liszewski, M. Kolev, G. Le Friec, M. Leung, P.G. Bertram, A.F. Fara, M. Subias, M.C. Pickering, C. Drouet, S. Meri, T.P. Arstila, P.T. Pekkarinen, M. Ma, A. Cope, T. Reinheckel, S. Rodriguez de Cordoba, B. Afzali, J.P. Atkinson, C. Kemper, Intracellular complement activation sustains T cell homeostasis and mediates effector differentiation, Immunity 39 (6) (2013) 1143–1157.

[68] M. von Essen, M.W. Nielsen, C.M. Bonefeld, L. Boding, J.M. Larsen, M. Leitges, G. Baier, N. Odum, C. Geisler, Protein kinase C (PKC) alpha and PKC theta are the major PKC isotypes involved in TCR down-regulation, J. Immunol. 176 (12) (2006) 7502–7510.

[69] Y. Xiong, W. Piao, C.C. Brinkman, L. Li, J.M. Kulinski, A. Olivera, A. Cartier, T. Hla, K.L. Hippen, B.R. Blazar, S.R. Schwab, J.S. Bromberg, CD4 T cell sphingosine 1-phosphate receptor (S1PR)1 and S1PR4 and endothelial S1PR2 regulate afferent lymphatic migration, Science Immunology 4 (33) (2019) eaav1263.

[70] S. Sakaguchi, N. Mikami, J.B. Wing, A. Tanaka, K. Ichiyama, N. Ohkura, Regulatory T cells and human disease, Annu. Rev. Immunol. 38 (1) (2020) 541–566.

[71] J. Ren, L. Han, J. Tang, Y. Liu, X. Deng, Q. Liu, P. Hao, X. Feng, B. Li, H. Hu, H. Wang, Foxp1 is critical for the maintenance of regulatory T-cell homeostasis and suppressive function, PLoS Biol. 17 (5) (2019) e3000270.

[72] F. Takizawa, J.M. Dijkstra, P. Kotterba, T. Korytář, H. Kock, B. Köllner, B. Jaureguiberry, T. Nakanishi, U. Fischer, The expression of CD8α discriminates distinct T cell subsets in teleost fish, Dev. Comp. Immunol. 35 (7) (2011) 752–763.

[73] C. Aquilino, R. Castro, U. Fischer, C. Tafalla, Transcriptomic responses in rainbow trout gills upon infection with viral hemorrhagic septicemia virus (VHSV), Dev. Comp. Immunol. 44 (1) (2014) 12–20.

[74] R. Yazawa, G.A. Cooper, M. Beetz-Sargent, A. Robb, L. McKinnel, W.S. Davidson, B.F. Koop, Functional adaptive diversity of the Atlantic salmon T-cell receptor gamma locus, Mol. Immunol. 45 (8) (2008) 2150–2157.

[75] J.C. Ribot, N. Lopes, B. Silva-Santos, γδ T cells in tissue physiology and surveillance, Nat. Rev. Immunol. 21 (4) (2021) 221–232.

[76] H. Melichar, K. Narayan, S. Der, Y. Hiraoka, N. Gardiol, G. Jeannet, W. Held, C. Chambers, J. Kang, Regulation of versus T lymphocyte differentiation by the transcription factor SOX13, Science (New York, N.Y.) 315 (2007) 230–233.

[77] N.A. Spidale, K. Sylvia, K. Narayan, B. Miu, M. Frascoli, H.J. Melichar, W. Zhihao, J. Kisielow, A. Palin, T. Serwold, P. Love, M. Kobayashi, M. Yoshimoto, N. Jain, J. Kang, Interleukin-17-Producing γδ T cells originate from SOX13(+) progenitors that are independent of γδTCR signaling, Immunity 49 (5) (2018) 857–872.e5.

[78] I.C. Ho, P. Vorhees, N. Marin, B.K. Oakley, S.F. Tsai, S.H. Orkin, J.M. Leiden, Human GATA-3: a lineage-restricted transcription factor that regulates the expression of the T cell receptor alpha gene, EMBO J. 10 (5) (1991) 1187–1192.

[79] S.K. Nandakumar, K. Johnson, S.L. Throm, T.I. Pestina, G. Neale, D.A. Persons, Low-level GATA2 overexpression promotes myeloid progenitor self-renewal and blocks lymphoid differentiation in mice, Exp. Hematol. 43 (7) (2015) 565–577, e1-10.

[80] J.A. Walker, P.A. Clark, A. Crisp, J.L. Barlow, A. Szeto, A.C.F. Ferreira, B.M. J. Rana, H.E. Jolin, N. Rodriguez-Rodriguez, M. Sivasubramaniam, R. Pannell, J. Cruickshank, M. Daly, L. Haim-Vilmovsky, S.A. Teichmann, A.N.J. McKenzie, Polychromic reporter mice reveal unappreciated innate lymphoid cell progenitor heterogeneity and elusive ILC3 progenitors in bone marrow, Immunity 51 (1) (2019) 104–118.e7.

[81] N.C. Guslund, A.K. Krabberød, S.F. Nørstebø, M.H. Solbakken, K.S. Jakobsen, F.-E. Johansen, S.-W. Qiao, Lymphocyte subsets in Atlantic cod (Gadus morhua) interrogated by single-cell sequencing, Commun. Biol. 5 (1) (2022) 689.

[82] T. Yamaguchi, F. Takizawa, M. Furihata, V. Soto-Lampe, J.M. Dijkstra, U. Fischer, Teleost cytotoxic T cells, Fish Shellfish Immunol. 95 (2019) 422–439.

[83] Z. Wu, Y. Zheng, J. Sheng, Y. Han, Y. Yang, H. Pan, J. Yao, CD3+CD4-CD8- (Double-Negative) T cells in inflammation, immune disorders and cancer, Front. Immunol. 13 (2022).

[84] C. Chou, X. Zhang, C. Krishna, B.G. Nixon, S. Dadi, K.J. Capistrano, E.R. Kansler, M. Steele, J. Han, A. Shyu, J. Zhang, E.G. Stamatiades, M. Liu, S. Li, M.H. Do, C. Edwards, D.S. Kang, C.-T. Chen, I.H. Wei, E.P. Pappou, M.R. Weiser, J. Garcia-Aguilar, J.J. Smith, C.S. Leslie, M.O. Li, Programme of self-reactive innate-like T cell-mediated cancer immunity, Nature 605 (7908) (2022) 139–145.

[85] V. Muncan, A. Faro, A.-P.G. Haramis, A.F.L. Hurlstone, E. Wienholds, J. van Es, J. Korving, H. Begthel, D. Zivkovic, H. Clevers, T-cell factor 4 (Tcf7l2) maintains proliferative compartments in zebrafish intestine, EMBO Rep. 8 (10) (2007) 966–973.

[86] A.P. Ng, S.J. Loughran, D. Metcalf, C.D. Hyland, C.A. de Graaf, Y. Hu, G.K. Smyth, D.J. Hilton, B.T. Kile, W.S. Alexander, Erg is required for self-renewal of hematopoietic stem cells during stress hematopoiesis in mice, Blood 118 (9) (2011) 2454–2461.

[87] E.L. Wuebben, S.K. Mallanna, J.L. Cox, A. Rizzino, Musashi2 is required for the self-renewal and pluripotency of embryonic stem cells, PLoS One 7 (4) (2012) e34827.

[88] M. Gleimer, H. Von Boehmer, T. Kreslavsky, PLZF controls the expression of a limited number of genes essential for NKT cell function, Front. Immunol. 3 (2012).

[89] M.G. Constantinides, B.D. McDonald, P.A. Verhoef, A. Bendelac, A committed precursor to innate lymphoid cells, Nature 508 (7496) (2014) 397–401.

[90] W. de Haan, C. Oie, M. Benkheil, W. Dheedene, S. Vinckier, G. Coppiello, X. L. Aranguren, M. Beerens, J. Jaekers, B. Topal, C. Verfaillie, B. Smedsrod, A. Luttun, Unraveling the transcriptional determinants of liver sinusoidal endothelial cell specialization, Am. J. Physiol. Gastrointest. Liver Physiol. 318 (4) (2020) G803–G815.

[91] A. Bottos, E. Destro, A. Rissone, S. Graziano, G. Cordara, B. Assenzio, M.R. Cera, L. Mascia, F. Bussolino, M. Arese, The synaptic proteins neurexins and neuroligins are widely expressed in the vascular system and contribute to its functions, Proc. Natl. Acad. Sci. U.S.A. 106 (49) (2009) 20782–20787.

[92] G. Haraldsen, D. Kvale, B. Lien, I.N. Farstad, P. Brandtzaeg, Cytokine-regulated expression of E-selectin, intercellular adhesion molecule-1 (ICAM-1), and vascular cell adhesion molecule-1 (VCAM-1) in human microvascular endothelial cells, J. Immunol. 156 (7) (1996) 2558–2565.

[93] S.K. Sinha, A. Miikeda, Z. Fouladian, M. Mehrabian, C. Edillor, D. Shih, Z. Zhou, M.K. Paul, S. Charugundla, R.C. Davis, T.B. Rajavashisth, A.J. Lusis, Local M-CSF (macrophage colony-stimulating factor) expression regulates macrophage proliferation and apoptosis in atherosclerosis, Arterioscler. Thromb. Vasc. Biol. 41 (1) (2021) 220–233.

[94] J. Kalucka, L.P.M.H. de Rooij, J. Goveia, K. Rohlenova, S.J. Dumas, E. Meta, N. V. Conchinha, F. Taverna, L.-A. Teuwen, K. Veys, M. García-Caballero, S. Khan, V. Geldhof, L. Sokol, R. Chen, L. Treps, M. Borri, P. de Zeeuw, C. Dubois, T. K. Karakach, K.D. Falkenberg, M. Parys, X. Yin, S. Vinckier, Y. Du, R.A. Fenton, L. Schoonjans, M. Dewerchin, G. Eelen, B. Thienpont, L. Lin, L. Bolund, X. Li, Y. Luo, P. Carmeliet, Single-cell transcriptome atlas of murine endothelial cells, Cell 180 (4) (2020) 764–779.e20.

[95] K.L. Betterman, D.L. Sutton, G.A. Secker, J. Kazenwadel, A. Oszmiana, L. Lim, N. Miura, L. Sorokin, B.M. Hogan, M.L. Kahn, H. McNeill, N.L. Harvey, Atypical cadherin FAT4 orchestrates lymphatic endothelial cell polarity in response to flow, J. Clin. Invest. 130 (6) (2020) 3315–3328.

[96] J.M. Smith, J.H. Meinkoth, T. Hochstatter, K.M. Meyers, Differential distribution of von Willebrand factor in canine vascular endothelium, Am. J. Vet. Res. 57 (5) (1996) 750–755.

[97] I. Buschmann, A. Pries, B. Styp-Rekowska, P. Hillmeister, L. Loufrani, D. Henrion, Y. Shi, A. Duelsner, I. Hoefer, N. Gatzke, H. Wang, K. Lehmann, L. Ulm, Z. Ritter, P. Hauff, R. Hlushchuk, V. Djonov, T. van Veen, F. le Noble, Pulsatile shear and Gja5 modulate arterial identity and remodeling events during flow-driven arteriogenesis, Development 137 (13) (2010) 2187–2196.

[98] S.J. Dumas, E. Meta, M. Borri, Y. Luo, X. Li, T.J. Rabelink, P. Carmeliet, Phenotypic diversity and metabolic specialization of renal endothelial cells, Nat. Rev. Nephrol. 17 (7) (2021) 441–464.

[99] J.R. Shutter, S. Scully, W. Fan, W.G. Richards, J. Kitajewski, G.A. Deblandre, C. R. Kintner, K.L. Stark, Dll4, a novel Notch ligand expressed in arterial endothelium, Genes Dev. 14 (11) (2000) 1313–1318.

[100] H.U. Wang, Z.F. Chen, D.J. Anderson, Molecular distinction and angiogenic interaction between embryonic arteries and veins revealed by ephrin-B2 and its receptor Eph-B4, Cell 93 (5) (1998) 741–753.

[101] N.D. Lawson, B.M. Weinstein, Arteries and veins: making a difference with zebrafish, Nat. Rev. Genet. 3 (9) (2002) 674–682.

[102] J.A. Fretz, T. Nelson, H. Velazquez, Y. Xi, G.W. Moeckel, M.C. Horowitz, Early B-cell factor 1 is an essential transcription factor for postnatal glomerular maturation, Kidney Int. 85 (5) (2014) 1091–1102.

[103] R.N. Hanna, L.M. Carlin, H.G. Hubbeling, D. Nackiewicz, A.M. Green, J.A. Punt, F. Geissmann, C.C. Hedrick, The transcription factor NR4A1 (Nur77) controls bone marrow differentiation and the survival of Ly6C- monocytes, Nat. Immunol. 12 (8) (2011) 778–785.

[104] H.M. Chen, P. Zhang, M.T. Voso, S. Hohaus, D.A. Gonzalez, C.K. Glass, D. E. Zhang, D.G. Tenen, Neutrophils and monocytes express high levels of PU.1 (Spi-1) but not Spi-B, Blood 85 (10) (1995) 2918–2928.

[105] A. Schüler, M. Schwieger, A. Engelmann, K. Weber, S. Horn, U. Müller, M. A. Arnold, E.N. Olson, C. Stocking, The MADS transcription factor Mef2c is a pivotal modulator of myeloid cell fate, Blood 111 (9) (2008) 4532–4541.

[106] T. Tsuruta, K. Tani, M. Shimane, K. Ozawa, S. Takahashi, D. Tsuchimoto, K. Takahashi, S. Nagata, N. Sato, S. Asano, Effects of myeloid cell growth factors on alkaline phosphatase, myeloperoxidase, defensin and granulocyte colony-stimulating factor receptor mRNA expression in haemopoietic cells of normal individuals and myeloid disorders, Br. J. Haematol. 92 (1) (1996) 9–22.
[107] N. Palha, F. Guivel-Benhassine, V. Briolat, G. Lutfalla, M. Sourisseau, F. Ellett, C. H. Wang, G.J. Lieschke, P. Herbomel, O. Schwartz, J.P. Levraud, Real-time whole-body visualization of Chikungunya Virus infection and host interferon response in zebrafish, PLoS Pathog. 9 (9) (2013) e1003619.
[108] D. Riyapa, D. Rinchai, V. Muangsombut, C. Wuttinontananchai, M. Toufiq, D. Chaussabel, M. Ato, J.M. Blackwell, S. Korbsrisate, Transketolase and vitamin B1 influence on ROS-dependent neutrophil extracellular traps (NETs) formation, PLoS One 14 (8) (2019) e0221016.
[109] A. Regev, S.A. Teichmann, E.S. Lander, I. Amit, C. Benoist, E. Birney, B. Bodenmiller, P. Campbell, P. Carninci, M. Clatworthy, H. Clevers, B. Deplancke, I. Dunham, J. Eberwine, R. Eils, W. Enard, A. Farmer, L. Fugger, B. Göttgens, N. Hacohen, M. Haniffa, M. Hemberg, S. Kim, P. Klenerman, A. Kriegstein, E. Lein, S. Linnarsson, E. Lundberg, J. Lundeberg, P. Majumder, J. C. Marioni, M. Merad, M. Mhlanga, M. Nawijn, M. Netea, G. Nolan, D. Pe'er, A. Phillipakis, C.P. Ponting, S. Quake, W. Reik, O. Rozenblatt-Rosen, J. Sanes, R. Satija, T.N. Schumacher, A. Shalek, E. Shapiro, P. Sharma, J.W. Shin, O. Stegle, M. Stratton, M.J.T. Stubbington, F.J. Theis, M. Uhlen, A. van Oudenaarden, A. Wagner, F. Watt, J. Weissman, B. Wold, R. Xavier, N. Yosef, The human cell atlas, Elife 6 (2017).
[110] N. Kim, H. Kang, A. Jo, S.A. Yoo, H.O. Lee, Perspectives on single-nucleus RNA sequencing in different cell types and tissues, J Pathol Transl Med 57 (1) (2023) 52–59.
[111] T.S. Andrews, J. Atif, J.C. Liu, C.T. Perciani, X.-Z. Ma, C. Thoeni, M. Slyper, G. Eraslan, A. Segerstolpe, J. Manuel, S. Chung, E. Winter, I. Cirlan, N. Khuu, S. Fischer, O. Rozenblatt-Rosen, A. Regev, I.D. McGilvray, G.D. Bader, S. A. MacParland, Single-cell, single-nucleus, and spatial RNA sequencing of the human liver identifies cholangiocyte and mesenchymal heterogeneity, Hepatology Communications 6 (4) (2022) 821–840.
[112] M. Slyper, C.B.M. Porter, O. Ashenberg, J. Waldman, E. Drokhlyansky, I. Wakiro, C. Smillie, G. Smith-Rosario, J. Wu, D. Dionne, S. Vigneau, J. Jané-Valbuena, T. L. Tickle, S. Napolitano, M.-J. Su, A.G. Patel, A. Karlstrom, S. Gritsch, M. Nomura, A. Waghray, S.H. Gohil, A.M. Tsankov, L. Jerby-Arnon, O. Cohen, J. Klughammer, Y. Rosen, J. Gould, L. Nguyen, M. Hofree, P.J. Tramontozzi, B. Li, C.J. Wu, B. Izar, R. Haq, F.S. Hodi, C.H. Yoon, A.N. Hata, S.J. Baker, M.L. Suvà, R. Bueno, E. H. Stover, M.R. Clay, M.A. Dyer, N.B. Collins, U.A. Matulonis, N. Wagle, B. E. Johnson, A. Rotem, O. Rozenblatt-Rosen, A. Regev, A single-cell and single-nucleus RNA-Seq toolbox for fresh and frozen human tumors, Nat. Med. 26 (5) (2020) 792–802.
[113] D.R. Farnsworth, L.M. Saunders, A.C. Miller, A single-cell transcriptome atlas for zebrafish development, Dev. Biol. 459 (2) (2020) 100–108.
[114] Q. Tang, S. Iyer, R. Lobbardi, J.C. Moore, H. Chen, C. Lareau, C. Hebert, M. L. Shaw, C. Neftel, M.L. Suva, C.J. Ceol, A. Bernards, M. Aryee, L. Pinello, I. A. Drummond, D.M. Langenau, Dissecting hematopoietic and renal cell heterogeneity in adult zebrafish at single-cell resolution using RNA sequencing, J. Exp. Med. 214 (10) (2017) 2875–2887.
[115] E. Denisenko, B.B. Guo, M. Jones, R. Hou, L. de Kock, T. Lassmann, D. Poppe, O. Clément, R.K. Simmons, R. Lister, A.R.R. Forrest, Systematic assessment of tissue dissociation and storage biases in single-cell and single-nucleus RNA-seq workflows, Genome Biol. 21 (1) (2020) 130.
[116] L. Jiménez-Gracia, D. Marchese, J.C. Nieto, G. Caratù, E. Melón-Ardanaz, V. Gudiño, S. Roth, K. Wise, N.K. Ryan, K.B. Jensen, X. Hernando-Momblona, J. P. Bernardes, F. Tran, L.K. Sievers, S. Schreiber, M. van den Berge, T. Kole, P. L. van der Velde, M.C. Nawijn, P. Rosenstiel, E. Batlle, L.M. Butler, I.A. Parish, J. Plummer, I. Gut, A. Salas, H. Heyn, L.G. Martelotto, FixNCut: single-cell genomics through reversible tissue fixation and dissociation, bioRxiv (2023), 2023.06.16.545221.
[117] J.-M. Oh, M. An, D.-S. Son, J. Choi, Y.B. Cho, C.E. Yoo, W.-Y. Park, Comparison of cell type distribution between single-cell and single-nucleus RNA sequencing: enrichment of adherent cell types in single-nucleus RNA sequencing, Exp. Mol. Med. 54 (12) (2022) 2128–2134.
[118] L.N.M. Harrahy, C.B. Schreck, A.G. Maule, Antibody-producing cells correlated to body weight in juvenile chinook salmon (Oncorhynchus tshawytscha) acclimated to optimal and elevated temperatures, Fish Shellfish Immunol. 11 (8) (2001) 653–659.
[119] M. Hashimoto, Y. Yamashita, N. Mori, Immunohistochemical detection of CD79a expression in precursor T cell lymphoblastic lymphoma/leukaemias, J. Pathol. 197 (3) (2002) 341–347.
[120] K.F. Bornhöfft, J. Martorell Ribera, T. Viergutz, M.T. Venuto, U. Gimsa, S. P. Galuska, A. Rebl, Characterization of sialic acid-binding immunoglobulin-type lectins in fish reveals teleost-specific structures and expression patterns, Cells 9 (4) (2020) 836.
[121] T. Wen, M.K. Mingler, C. Blanchard, B. Wahl, O. Pabst, M.E. Rothenberg, The pan-B cell marker CD22 is expressed on gastrointestinal eosinophils and negatively regulates tissue eosinophilia, J. Immunol. 188 (3) (2012) 1075–1082.
[122] P. Perdiguero, E. Morel, C. Tafalla, Diversity of rainbow trout blood B cells revealed by single cell RNA sequencing, Biology 10 (6) (2021) 511.
[123] G.T. Hart, X. Wang, K.A. Hogquist, S.C. Jameson, Krüppel-like factor 2 (KLF2) regulates B-cell reactivity, subset differentiation, and trafficking molecule expression, Proc. Natl. Acad. Sci. USA 108 (2) (2011) 716–721.
[124] V.S. Mahajan, H. Mattoo, N. Sun, V. Viswanadham, G.J. Yuen, H. Allard-Chamard, M. Ahmad, S.J.H. Murphy, A. Cariappa, Y. Tuncay, S. Pillai, B1a and B2 cells are characterized by distinct CpG modification states at DNMT3A-maintained enhancers, Nat. Commun. 12 (1) (2021) 2208.
[125] D. Bhattacharya, M.T. Cheah, C.B. Franco, N. Hosen, C.L. Pin, W.C. Sha, I. L. Weissman, Transcriptional profiling of antigen-dependent murine B cell differentiation and memory formation, J. Immunol. 179 (10) (2007) 6808–6819.
[126] N.R. Kong, M. Davis, L. Chai, A. Winoto, R. Tjian, MEF2C and EBF1 Co-regulate B cell-specific transcription, PLoS Genet. 12 (2) (2016) e1005845.
[127] U. Grimholt, A.Y.M. Sundaram, C.A. Bøe, M.K. Dahle, M. Lukacs, Tetraploid ancestry provided atlantic salmon with two paralogue functional T cell receptor beta regions whereof one is completely novel, Front. Immunol. 13 (2022).
[128] H.-f. Tian, J. Xing, X.-q. Tang, H. Chi, X.-z. Sheng, W.-b. Zhan, Cluster of differentiation antigens: essential roles in the identification of teleost fish T lymphocytes, Marine Life Science & Technology 4 (3) (2022) 303–316.
[129] A. Souabni, W. Jochum, M. Busslinger, Oncogenic role of Pax5 in the T-lymphoid lineage upon ectopic expression from the immunoglobulin heavy-chain locus, Blood 109 (1) (2006) 281–289.
[130] A.B. van Spriel, K.L. Puls, M. Sofi, D. Pouniotis, H. Hochrein, Z. Orinska, K. P. Knobeloch, M. Plebanski, M.D. Wright, A regulatory role for CD37 in T cell proliferation, J. Immunol. 172 (5) (2004) 2953–2961.
[131] Y. Zhou, J. Petrovic, J. Zhao, W. Zhang, A. Bigdeli, Z. Zhang, S.L. Berger, W. S. Pear, R.B. Faryabi, EBF1 nuclear repositioning instructs chromatin refolding to promote therapy resistance in T leukemic cells, Mol Cell 82 (5) (2022) 1003–1020 e15.
[132] J. Lovy, P. Piesik, P.K. Hershberger, K.A. Garver, Experimental infection studies demonstrating Atlantic salmon as a host and reservoir of viral hemorrhagic septicemia virus type IVa with insights into pathology and host immunity, Vet. Microbiol. 166 (1) (2013) 91–101.
[133] M. Aamelfot, O.B. Dale, S.C. Weli, E.O. Koppang, K. Falk, Expression of the infectious salmon anemia virus receptor on atlantic salmon endothelial cells correlates with the cell tropism of the virus, J. Virol. 86 (19) (2012) 10571–10578.
[134] T. Seternes, K. Sorensen, B. Smedsrod, Scavenger endothelial cells of vertebrates: a nonperipheral leukocyte system for high-capacity elimination of waste macromolecules, Proc Natl Acad Sci U S A 99 (11) (2002) 7594–7597.
[135] R. Gao, C. Kim, E. Sei, T. Foukakis, N. Crosetto, L.K. Chan, M. Srinivasan, H. Zhang, F. Meric-Bernstam, N. Navin, Nanogrid single-nucleus RNA sequencing reveals phenotypic diversity in breast cancer, Nat. Commun. 8 (1) (2017) 228.
[136] A. Subramanian, M. Alperovich, Y. Yang, B. Li, Biology-inspired data-driven quality control for scientific discovery in single-cell transcriptomics, Genome Biol. 23 (1) (2022) 267.
[137] E.I. Athanasiadis, J.G. Botthof, H. Andres, L. Ferreira, P. Lio, A. Cvejic, Single-cell RNA-sequencing uncovers transcriptional states and fate decisions in haematopoiesis, Nat. Commun. 8 (1) (2017) 2045.